

**HETEROGENEOUS PHOTOCATALYSIS OF
GLOVE WASTEWATER OVER GREEN
SYNTHESIZED ZNO IMMOBILIZED ON
NATURAL HYDROXYAPATITE**

LEOW GUO QUAN

UNIVERSITI TUNKU ABDUL RAHMAN

**HETEROGENEOUS PHOTOCATALYSIS OF GLOVE WASTEWATER
OVER GREEN SYNTHESIZED ZNO IMMOBILIZED ON NATURAL
HYDROXYAPATITE**

Leow Guo Quan

**A project report submitted in partial fulfilment of the requirements for the
award of Bachelor of Engineering (Hons) Petrochemical Engineering**

Faculty of Engineering and Green Technology

Universiti Tunku Abdul Rahman

May 2019

DECLARATION

I hereby declare that this project report is based on my original work except for citations and quotations which have been duly acknowledged. I also declare that it has not been previously and concurrently submitted for any other degree or award at UTAR or other institutions.

Signature : _____

Name : _____

ID No. : _____

Date : _____

APPROVAL FOR SUBMISSION

I certify that the project report entitled “Heterogeneous Photocatalysis of Glove Wastewater over Green Synthesized ZnO Immobilized on Natural Hydroxyapatite” was prepared by LEOW GUO QUAN has met the required standard for submission in partial fulfilment of the requirements for the award of Bachelor of Engineering (Hons) Petrochemical Engineering at Universiti Tunku Abdul Rahman.

Approved by,

Signature : _____

Supervisor : DR Sin Jin Chung

Date : _____

Signature : _____

Co-Supervisor: DR Lam Sze Mun

Date : _____

The copyright of this report belongs to the author under the terms of the copyright Act 1987 as qualified by Intellectual Property Policy of Universiti Tunku Abdul Rahman. Dues acknowledgement shall always be made of the use of any material contained in, or derived from, this report.

© 2019, Leow Guo Quan. All right reserved

Specially dedicated to

My beloved parents, supervisor, lecturers, seniors and friends

ACKNOWLEDGEMENTS

First and foremost, I would like to thank everyone who had contributed to the successful completion of this project. I would like to express my gratitude to my research supervisor, Ts. Dr Sin Jin Chung for this invaluable advice, guidance and his enormous patience throughout the development of the research. I am particularly grateful for his feedback and guidance throughout the entire course of the project.

Secondly, I would like to extend my thanks to the laboratory staffs of the petrochemical engineering department for their help in the usage of all the necessary instruments needed for this research.

In addition, I would also like to express my gratitude to my friends, seniors and lecturers who had helped and given me encouragement.

Lastly, I would also like to express my gratitude to my parents and siblings who have supported me during the development of this project.

HETEROGENOUS PHOTOCATALYSIS OF WASTEWATER FROM GLOVE INDUSTRY

ABSTRACT

Photocatalytic degradation of glove wastewater has been studied in this research to treat the ongoing water pollution from the glove industry. The green synthesized using plant extracts was emerged as a renewable, cost effectively and environmental friendly method that can be used to synthesis zinc oxide (ZnO) photocatalyst. Corn husk extract was used to synthesis ZnO without the usage of harmful chemicals. Besides that, the ZnO also coupled with the natural hydroxyapatite (HAp) that obtained from buffalo bone to enhance the photocatalysis. ZnO, HAp and ZnO/HAp was characterized through numerous analyses which included X-ray diffraction (XRD), scanning electron microscopy (SEM), energy dispersive X-ray (EDX), Fourier transform infrared spectroscopy (FTIR), Ultraviolet-visible diffuse reflectance spectroscopy (UV-vis DRS), and Particle Size Analysis (PSA). The ZnO was observed as hexagonal wurtzite structure and HAp was indicate in the XRD analysis. Green synthesized ZnO, HAp and ZnO/HAp was observed as porous and fluffy in nature in the SEM analysis. The fine particle of ZnO and ZnO/HAp was observed through PSA. EDX analysis determines the composition of element that presented in the photocatalyst. The content of HAp on the ZnO was studied in this research by varying 20 wt% to 50 wt % of HAp. The optimum HAp content on ZnO was ZnO-50%HAp was achieved 100 % photocatalytic degradation efficiency of glove wastewater. The effects of initial wastewater concentration and ZnO/HAp catalyst loading were studied. The optimal ZnO-50%HAp catalyst loading was found to be 1 g/L. Consequently, the effect of various scavengers was also investigated to determine the role of each active species in the reaction mechanism. The h^+ radicals was observed to be the main reactive species in this study.

TABLE OF CONTENTS

DECLARATION	ii
APPROVAL FOR SUBMISSION	iv
ACKNOWLEDGEMENTS	vi
ABSTRACT	vii
TABLE OF CONTENTS	viii
LIST OF TABLE	xi
LIST OF FIGURES	xii
LIST OF SYMBOLS/ABBREVIATIONS	xiv
LIST OF APPENDIXES	xvi

CHAPTER

1	INTRODUCTION	
	1.1 Background	1
	1.2 Problem Statement	7
	1.3 Objectives	11
	1.4 Scope of Study	11
2	LITERATURE REVIEW	
	2.1 ZnO as Photocatalyst	12
	2.1.1 Introduction of ZnO	12
	2.1.2 Semiconductors ZnO	16

2.2	Principles of mechanism of ZnO photocatalyst	17
2.2.1	Mechanism of ZnO Photocatalyst	18
2.3	Green Synthesized of ZnO nanomaterial	20
2.4	ZnO supported on hydroxyapatite (ZnO/Hap)	26
2.5	Review on the glove wastewater	30
2.6	Photocatalyst Degradation of the Rubber Wastewater	34
2.7	Effect of operating parameter	37
2.7.1	Effect of Photocatalyst Loading	37
3	METHODOLOGY	40
3.1	Overall Flowchart of the Work	40
3.2	Material and Chemicals	41
3.3	Photocatalytic Degradation Experiment Setup	42
3.4	Preparation of ZnO-supported Hap photocatalyst	43
3.4.1	Preparation of green extracts	43
3.4.2	Preparation of Green synthesized corn husk ZnO	44
3.4.3	Preparation of Bone Derived Photocatalyst	45
3.4.4	Preparation of Green Synthesized ZnO/HAp	46
3.5	Characterization of Photocatalyst	47
3.5.1	X-Ray Diffraction (XRD)	47
3.5.2	Scanning Electron Microscopy (SEM) and Energy Dispersion X-Ray (EDX)	47
3.5.3	Fourier Transform Infrared Spectroscopy (FTIR)	47
3.5.4	Ultraviolet-visible Diffuse Reflectance Spectroscopy (UV-vis DRS)	48
3.5.5	Particle Size Analysis (PSA)	48
3.6	Photocatalytic Activity	48
3.7	Effect of HAp weight percent on ZnO/HAp nanoparticles	49
3.7.1	Effect of Catalyst Loading	49
3.7.2	Scavenger Test	50
3.8	Phytotoxicity Testing	50
4	RESULTS AND DISCUSSION	51

4.1	Characterization	51
4.1.1	X-ray Diffraction (XRD)	51
4.1.2	Scanning Electron Microscopy (SEM)	53
4.1.3	Energy Dispersion X-ray (EDX)	54
4.1.4	Fourier Transform Infrared Spectroscopy (FTIR)	56
4.1.5	Ultraviolet-visible Diffuse Reflectance Spectroscopy (UV-vis DRS)	58
4.1.6	Particle Size Analysis	60
4.2	Control Experiment	62
4.3	Effect of Hap Content in ZnO	64
4.4	Radical Scavenger Test	66
4.5	Phytotoxicity	69
4.6	Effect of Operating Parameter	71
4.6.1	Effect of initial wastewater concentration	71
4.6.2	Effect of Photocatalyst Loading	73
4.7	Glove Wastewater Characteristic	75
5	CONCLUSION AND RECOMMENDATION	77
5.1	Conclusion	77
5.2	Recommendation	79
	REFERENCES	80
	APPENDICES	93

LIST OF TABLES

TABLE	TITLE	PAGE
2.1	VB (valence band); CB (conduction band); and Eg (band gap energy).	16
2.2	List of Organic pollutants degradable by ZnO photocatalyst	19
2.3	The green synthesized of ZnO through the different leaf and fruit extract	23
2.4	The green Synthesized of ZnO through the fruit extract	25
2.5	Hydroxyapatite as a Catalyst Support	29
2.6	The characteristic of rubber wastewater	30
2.7	Limits of Effluent of Standards A and B	32
2.8	The research paper on the characteristic of rubber wastewater	33
2.9	Examples of non-photochemical AOPS	35
2.10	Effect of photocatalyst loading on the Photocatalytic Degradation	39
3.1	List of chemicals and materials utilized in this study	41
4.1	Refractive Index	60
4.2	Physical Properties of Photocatalyst	61
4.3	Glove Wastewater Characteristic	75

LIST OF FIGURES

FIGURE	TITLE	PAGE
2.1	Three different atomic structure of ZnO (a) zincblende, (b) wurtzite and (c) rocksalt structures.	14
3.1	General Flow Chart of the work	40
3.2	Schematic Diagram of the Photocatalysis System under UV-c irradiation	42
3.3	Flow Chart of preparation of green extracts	43
3.4	Flow Chart of preparation of ZnO	44
3.5	Flow chart preparation of Bone derived photocatalyst (Hydroxyapatite)	45
3.6	Flow Chart of Preparation of green synthesized ZnO/HAp	46
4.1	XRD pattern of ZnO, HAp, and ZnO-50%HAp	52
4.2	SEM image of Green Synthesized	54
4.3	EDX spectrum of Green Synthesized	55
4.4	FTIR result of ZnO, HAp, ZnO-50%HAp	57
4.5	UV-vis DRS Spectrum of Buffalo Bone HAp	58
4.6	UV-vis DRS Spectrum of Green Synthesized Corn Husk ZnO	59
4.7	UV-vis DRS Spectrum of ZnO-50%HAp	59
4.8	Particle Size Analysis	60
4.9	Photocatalytic Degradation of Glove Wastewater under different conditions	62
4.10	Effect of Hap content in ZnO/Hap nanocomposites for photocatalytic degradation of glove wastewater	64
4.11	Effect of Different Scavengers at 0.5Mm on photocatalytic degradation of glove wastewater over ZnO nanocomposites	67

4.12	Phytotoxicity Test	69
4.13	Effect of Initial Wastewater Concentration on the photocatalytic degradation of glove wastewater over ZnO/HAP nanocomposites	71
4.14	Effect of Catalyst Loading on Photocatalytic Degradation of Glove Wastewater over ZnO/HAP nanocomposites	74

LIST OF SYMBOLS/ABBREVIATIONS

$\cdot OH$	Hydroxyl Radicals
C_0	Concentration of pollutant after 30 min of dark run, mg/L
C_t	Concentration at the reaction time(t), mg/L
t	Reaction time, min
c	Light velocity, m/s
h	Planck's constant, eV
$h\nu$	Photon energy, eV
λ	Wavelength of adsorption, nm
E_g	Band Gap Energy
1-D	One-Dimensional
3-D	Three-Dimensional
AOP	Advanced Oxidation Process
C	Carbon
CB	Conduction Band
CO ₂	Carbon Dioxide
CdS	Cadmium Sulphite
C ₂ H ₅ OH	Ethanol
O ₃	Ozone
$\cdot O_2^-$	Superoxide anion radical
H ₂ O ₂	Hydrogen Peroxide

OH·	Hydroxyl Radical
UV	Ultraviolet Radiation
ZnO	Zinc Oxide
TiO ₂	Titanium Oxide
Fe ₂ O ₃	Iron(II) Oxide
WO ₃	Tungsten Trioxide
HAp	Hydroxyapatite
BOD	Biological Oxygen Demand
COD	Chemical Oxygen Demand
TSS	Total Suspended Solid
XRD	X-Ray Diffraction
SEM	Scanning Electron Microscope
EDX	Energy Dispersive X-Ray Spectroscopy
TEM	Transmission Electron Microscopy
WZ	Wurtzite
ZB	Zinc Blende
CB	Conduction Band
VB	Valance Band
tr	trapped charge particles
HO ₂	Hydroperoxyl Radicals (HO ₂)
ZnO	Zinc Oxide
HAp	Hydroxyapatite
ppm	Part Per Million
g/L	Gram per litre
C/C ₀	Concentration /initial concentration

LIST OF APPENDIXES

APPENDIX	TITLE	PAGE
A	SEM image of Corn Husk ZnO with different magnification	87
B	SEM image of HAp with different magnification	88
C	SEM image of ZnO-20%HAp with different magnification	89
D	SEM image of ZnO-30%HAp with different magnification	90
E	SEM image of ZnO-40%HAp with different magnification	91
F	SEM image of ZnO-50%HAp with different magnification	92

CHAPTER 1

INTRODUCTION

1.1 Background of study

In recent years, continuous development of the industries and technologies leads to the environmental pollution. The water pollution is one of the important issues due to the emerging of the manufacturing industry. Water is the most essential natural resource for all living organisms and also the most valuable asset on earth. Besides that, water is the prime element of the life and human body also consists of 75 % of water. Nevertheless, water has been classified as the freshwater from the world's total water resources, is gradually decreasing with the emerging of the industries and technologies. Therefore, the quality of the water is the major concern of the government authorities and non-government authorities too. Water pollution can be defined by the exceeding amount of toxic chemical and biological agents that present in water bodies such as ground water, rivers, lakes and oceans. (Environmental Pollution Centres, 2017). The presence of the toxic chemical and biological agent will change the physical properties, chemical properties and biological properties of the water and will have a detrimental consequence on the living organisms and environment. The water pollution will lead to destruction of ecosystem which causes the ecosystem to collapse and bring harmful effect to our daily life since water is the most important and natural resource on the planet.

Water pollution can be categorised into two different sources which are point sources and non-point sources. The point sources mean the sources that can be

recognised, controlled and monitored easily, whereas non-point sources are difficult to control. The point sources are also known as direct sources which are normally from the manufacturing industries, waste management facilities, refineries, and sewage treatment plant. Whereas, indirect sources are the sources that are hard to be controlled, which is the pollutant enters the water bodies via ground water or soil or via the atmosphere as acid rain. According to the report of department of environment (2012), 1,662,329 water pollution point sources were identified, which comprised of 4,595 manufacturing industries, 9,883 sewage treatment plants (not including individual and communal septic tanks), 754 animal farm (pig farming), 508 agro-based industries, 865 wet markets and 192,710 food services establishments (Department of Environment, 2012). Therefore, the manufacturing industries play the most important role to reduce water pollution. The manufacturing industries wastewater are often contaminated with metals, toxic, chemical, petroleum products and other pollutants that are harmful to water sources. In Malaysia, the Environment Quality Act 1974 is an act that used for prevention, control of pollution and enhancement of the environment (Elaw, 2018). The discharge of the wastewater from any facility is required to have the permit from the Department of Environment. Even though this act restricts the waste discharged to the environment, the pollution issue still exists.

Malaysia is the primary rubber based product manufacturers in worldwide such as tyres and latex related product. Rubber based product industry in Malaysia contributes MYR 32.3 billion earnings in 2017 for exporting the rubber product, whereby rubber based product accounted for 30.2 % of Malaysia's overall exports for manufacturing products (Star, 2018). However, the emerging of the rubber based industry in these few years leads to a big issue which is generation of environmental damages. This is owing to the rubber industry which has large quantities of wastes and effluent as their by-product owing to the consuming of large amount of water, uses chemical and other utilities for manufacturing. Therefore, the waste and effluents discharge from the rubber based industry consume in large quantity. Thus, the water pollution in Malaysia can be majorly contributed from the rubber wastewater from the rubber based industry. The wastewater which is straight discharged into the water bodies likes wells, streams, rivers, lakes, oceans, and

ground without any pre-treatment will inevitably pollute the water sources. Discarding of the untreated effluent of the rubber based industry to the water bodies will result to the serious depletion of dissolved oxygen and affect the aquatic life inside the water bodies (Mohammadi.M, 2010). The effluent from the rubber-based industry includes of wash water, minor amounts of un-coagulated latex and serum which contain protein, carbohydrates, lipids, carotenoids and salts (Mohammadi.M, 2010). The serum effluents from the rubber manufacturing industry are mainly of the nitrogenous compound which will cause the will cause the algal bloom and result in the eutrophication of the water bodies.

With the sustainable development of the rubber based industry, the industry should eliminate and minimize the waste that discharged straight to the water bodies without any treatment which will result in the environmental pollution and any harmful effect to the living organisms. Manufacturing industry should focus on cleaner production technology, waste minimization, wastewater treatment, resources recovery and recycling of water sources. Wastewater treatment is commonly used to minimize and eliminate the waste and potential harm to the water bodies. The wastewater treatment is a method that utilized to treat the water sources that are no longer needed or no longer suitable to be used to clean water so that can be recovered or discharged to the environment (Conserve Energy Future, 2018). Wastewater treatment can be originated into biological treatment, physical treatment and chemical treatment. The biological treatment systems are more common to utilise for treating the household water and business premises to produce the water that is suitable for drinking purpose. It uses the biological matter and bacteria to collapse the waste matter and nutrients. The biological treatment is an important process which always treats the wastewater into the clean and fresh water for drinking purpose to avoid the harmful effect brings to our body. The method that is used for treating the wastewater from industries, factories and manufacturing firms is physical treatment system such as sedimentation, aeration and filtration are involved in the physical treatment process to treat the wastewater for making the water cleaner and quality better. (Amna, Adnan, 2010). The physical wastewater treatment systems use the chemical reaction as well as physical processes to treat wastewater. Owing to most of the wastewater from these industries contains chemical and others toxins that can bring the harmful effect to the environment and aquatic life. Chemical

wastewater treatment systems are utilising the chemical to treat the wastewater. The chemical treatment that most common for using to treat the industrial wastewater is called neutralization which utilises the base or acid to level its pH. The biological wastewater treatment process consumes high amount of energy. Furthermore, the biological wastewater treatment also requires large lands and higher maintenance cost. Therefore, the chemical treatment is more suitable for treating the large amount of water that discharged from the industry and factories daily. The continuous emerging of the chemical wastewater treatment provides the new environmentally friendly process to treat the wastewater without consuming high energy and lowers the emission of carbon dioxide (CO₂). The chlorination method that used for treating the wastewater is highly effective but the chlorine present which will bring the harmful effect to human health and safety risk for storage the large amount of chlorine which is toxic chemical. Therefore, the continuous development of the wastewater treatments technology by the researchers has been carried out with safer and also often more effective oxidation technique to treat the wastewater.

The chemical wastewater treatment technology that generated by the researchers with safer and also more effective oxidation technique is advanced oxidation processes (AOPs). AOPs has been developed which also emerges as the environmental friendly technology used for accelerating the oxidation and degradation of organic matters in wastewater. AOPs are to perform the wastewater treatment method which can be optimized the treatment and yield a product suitable for reclamation and reusable. AOPs are the processes that generate the significant amount of hydroxyl radical ($\cdot\text{OH}$) in the mechanism that leads to the degradation of target contaminants, which includes the organics, inorganics, metals and pathogens. AOPs combines the reagents such as ozone with $\text{OH}\cdot$ and ozone (O₃) with hydrogen peroxide H₂O₂ which will generate the $\text{OH}\cdot$ radicals as strong oxidants to oxidize the organic matters and inorganics contaminants inside the water bodies. AOPs are also used to increase the wastewater biodegradability which performs as the pre-treatment prior to an ensuing biological treatment. The commonly used advance oxidation processes to treat the manufacturing industries wastewater are using the fluorine, hydroxyl radical, ozone, hydrogen peroxide, chlorine, bromine and iodine.

AOPs is performed by different external energy sources such as electricity, ultraviolet irradiation (UV) or sun light. Moreover, AOPs have been developed into different type of methods that are used to treat the wastewater includes the homogenous and heterogeneous photocatalytic processes. Photocatalytic process is the type of advanced oxidation processes that involve catalytic reactions that proceed under the effect of light which also known as the light driven AOPs. Photocatalytic reaction is performing under presence of catalyst, light energy and oxygen sources. Photocatalytic reaction is carried out by formation of strong oxidants such as ozone, hydrogen peroxide and photocatalyst is often used at the same time for the generation of hydroxyl radical. Catalyst that used in conventional catalysis is activated by heat. Therefore, the photocatalyst is activated under irradiation of ultraviolet light to generate powerful oxidants. Advantage of utilising the photocatalytic process is its auto-cleaning effects which reduce the material conservation and maintenance cost. Owing to photocatalyst will avoid the deposition of dust/dirt on photocatalyst surface in greater extent than in photocatalyst surfaces not treated and also reduce the odours of the biocide and organoleptic character. (Melanie, R., 2010)

Heterogeneous photocatalysis is a technology that accelerates the photoreaction in the presence of catalyst. Heterogeneous photocatalysis performs the degradation of organic pollutant or photoreaction which is controlled by combined actions of a photocatalyst, light energy, and oxidizing agents. Light sources with semiconductor catalyst is utilized to initiate the photoreaction and conduct oxidation and reductions simultaneously. Heterogeneous photocatalytic uses semiconductors catalyst for removing organic species in the water pollutant and acts as an electrode. The heterogeneous photocatalysis can be used to degrade the organic pollutant to generate Carbon dioxide and water through $\text{OH}\cdot$ radicals attack in the bulk solution and direct H_+ oxidation on the semiconductor catalyst surface as compared with conventional treatment. The semiconductor catalysts that commonly used for photocatalytic process are ZnO , TiO_2 , Fe_2O_3 , and WO_3 . The semiconductor catalysts such as ZnO and WO_3 are most probably used in photocatalysis reaction. This is owing to their advantages such as low cost and good chemical stability (Akkari et al, 2018). The photocatalyst with wide band gap energy is better than the low band gap

which has higher free energy of photo generated charge carriers formed, low chemical and photochemical stability.

In recent years, the semiconductor that most probably used as the photocatalyst for degradation of emerging pollutant in wastewater is Zinc Oxide (ZnO) among the others owing to its extraordinary physical properties that function well in heterogeneous photocatalysis. ZnO is a semiconductor with excellent physiochemical and wide band gap showing good optoelectronic, catalytic, excellent photochemical properties. ZnO is also a semiconductor with low cost, excellent UV shielding property, environmental stability and nontoxicity. (Akkari et al., 2018). With the sustainable development, ZnO can be prepared by several structures with a several type of morphologies structures such as nanorods, nanocuboids, hierarchical and complex ZnO microarchitectures to perform better with different type of wastewater to be treated (Lam et al., 2018).

The ZnO nanoparticles are normally synthesised through physical and chemical method. Different methods that used to synthesize the ZnO nanoparticles through physical and chemical method such as thermal evaporation, sol-gel, wet chemical solution, hydrothermal, and template assisted growth. With the sustainable development, the Advanced Oxidation Processes is going toward the direction of 'Green'. The physical and chemical method are no longer chosen to be used because these methods consume a lot of energy and non-environmental friendly chemical reagents, which may cause harmful effect to nature. The development of eco-friendly synthesised methods is through the green synthesised of nanoparticles. Green synthesised are able to overcome the problems from physical and chemicals method. The green synthesised of nanoparticles is using the plant extracts which are the cleanest, biocompatible, and eco-friendly methods for large-scale production of nanomaterials (Karthik et al., 2017). The plant extracts are suitable to be used for green synthesised owing to the main components inside the plant extracts which consist of poly-ol, which can stabilize the formation of metallic nanoparticles and act as a chelating and capping agent for speedy biosynthesised of nanomaterials. (Karthik et al., 2017). The semiconductors catalysts that fabricated through the green synthesised routes are performed with excellent structure and better physiochemical

properties. Modification of ZnO with hydroxyapatite (Hap) was reported as a promising way to develop its photocatalytic activity. Hydroxyapatite (Hap) is a calcium phosphate as well as the human hard tissue in morphology and composition. The hydroxyapatite is used as a support for the semiconductor catalyst to perform the photocatalysis reaction. This is owing to the stability of the hydroxyapatite, strong adsorption capability, surface acidity/basicity and ion exchange ability (Fluidinova, 2018).

1.2 Problem Statement

The rubber based industry is emerging in the world in recent years especially in Asia and this sector also provides significant benefits for human being by manufacturing different kind of important rubber goods. However, water that discharged from this sector is one of the major environment problems that faced by the world. Owing to the rubber based industry consumes large amount of water and energy, large amount of chemical and other utilities which will generate significant amount of waste and effluents. The water pollution issues are caused by the wastewater that discharged from rubber glove industry or latex industry that used for production process and washing of the maturation container that contains suspended latex particles. The maturation process is the pre-treatment of rubber latex by chemicals. The large amount of the suspended solid that cannot be wiped off easily during the process makes it highly polluted. The wastewater discharged from the rubber based industry normally contains high biological oxygen demand (BOD) and ammonia. The high concentration of ammonia present in the wastewater effluent without any treatment will cause the harmful effect to the aquatic organisms. Besides that, the acidic effluent is also one of the major effluents that discharged from the rubber industry owing to the utilisation of acid in latex coagulation. Therefore, the acidic effluent mainly consists of carbonaceous organics material, nitrogen, and sulphate.

In the glove industry, the four sources of water effluent that used to clean the gloves are glove former cleaning tank, latex dipping tank, leaching tank, and latex compounding tank. The glove former cleaning tank consists of acid tank and alkali

tank which collect the acid and alkali to clean the former. Furthermore, the leaching tank is used for removing the chemical and protein from the gloves. The latex dipping and compounding tank contain the wastewater from the latex container, uncoagulated latex and sludge. The effluent from these 4 sources that discharged to the water bodies contains high concentration of organic matters which will cause and led to serious water pollution and killed the aquatic organism. Therefore, the conventional wastewater treatment must be applied inside the glove or rubber based industry prior the discharge of wastewater to the water bodies. The wastewater treatments that are commonly used can be categorized into physical, chemical, and biological wastewater treatment. Both of these method has its own disadvantages. Biological treatment requires large and takes longer time for treating the toxic substances inside the effluent owing to which can affect the growth of microorganism. The disadvantage of the physical treatment method is it requires large land area for the process which includes the sedimentation tank, aeration tank and filtration tank. Besides that, the cleaning of the physical treatment method is hassle and the temperature changes will affect the tank greatly. The conventional chemical wastewater treatment systems are utilising different types of chemical to treat the wastewater. Chlorine, ozone, and neutralisation method are the more common method that used for chemically treating the wastewater. However, conventional chemical and physical wastewater treatment method are not suggested to use owing to these methods consumed more energy, hazardous chemical reagents, high cause of chemical consumption, high labour cost, and high maintenance cost.

Therefore, the chemical wastewater treatment that is selected in this study to be used to treat the wastewater is Advanced oxidation processes (AOPs) because of its environmental friendly technology that are used for accelerating the degradation of a wide range of organic matters in wastewater. Nevertheless, these processes cannot completely eliminate the organic content present inside wastewater. Therefore, advanced oxidation processes have been developed into photocatalysis reaction. Photocatalysis also known as the light driven AOPs and it is performing in the presence of photocatalyst, oxygen sources, and light energy. The photocatalytic process relies on the production of hydroxyl radicals ($\text{OH}\cdot$) which has oxidant reduction potential to oxidize the organic compound present in water and perform the degradation under UV irradiation and its advantages is auto cleaning effect to reduce

the material conservation and maintenance cost. Photocatalyst will avoid the deposition of dirt/dust on photocatalyst surface in greater extent than in surfaces not treated and also reduce the odours of the biocide and organoleptic character. (Melanie, R., 2010). The photocatalysis processes perform well in the degradation of the water pollutant but these processes are expensive and consume large scale of energy. Hence, an environmental friendly and more economic method to perform the photocatalytic process may involve the use of heterogeneous photocatalysis. Heterogeneous photocatalysis is emerging as the promising wastewater treatment method as it performs well in degrading the aromatic compound which presents a potential hazard to water bodies. For the heterogeneous photocatalysis reaction, the semiconductor catalyst is utilized as an electrode for initiating the photoreaction and removing organic species in the water pollutant. The most common catalyst used for the heterogeneous photocatalysis reaction to treat the wastewater is TiO_2 owing to its excellent physical properties, high ultraviolet absorption, and high stability. However, the ZnO has been selected as a photocatalyst in our research. This is owing to ZnO is presented with the great interest to develop the novel photocatalysis and ZnO has higher wide gap band energy than TiO_2 . In general, wide band gap energy semiconductor catalyst is better than the low band gap semiconductor catalyst which has higher free energy of photo generated charge carriers formed, low chemical and photochemical stability. Besides that, ZnO is also showing good optoelectronic, piezoelectric, biocompatibility and photochemical stability. By comparing the ZnO and TiO_2 , the ZnO is able to absorb over a larger region of solar spectrum which enhance the efficiency of photocatalytic. Therefore, ZnO has been proven with better physical properties than TiO_2 to deserve as the better candidate for the photocatalysis of high organic content wastewater. ZnO takes the advantages of having the direct band gap energy (3.3eV), an excitation binding energy (60 meV than TiO_2 , 4meV), and can be synthesized easily in low temperature and different structure. (Roge et al., 2016).

ZnO can be synthesized through different methods or techniques. The physical and chemical syntheses are the conventional synthesis techniques of the ZnO semiconductor photocatalyst. The chemical synthesized technique such as sol-gel and hydrothermal synthesis method are the relatively easy methods for synthesizing ZnO particles into a narrow size distribution and outstanding

crystallinity. Though, chemical synthesis method requires high temperature and pressure for their initiation, whereas some methods require inert atmosphere protection. Besides that, the chemical synthesis technique that is used for stabilizing the ZnO nanoparticles consumed toxic will cause the production of non-eco-friendly by products (Sidra Sabir et al., 2014). Physical synthesis technique such as metal organic chemical vapour deposition employed at high temperature and low pressure. The green synthesis technique to synthesis the ZnO nanoparticles is emerging and reducing the use of physical and chemical syntheses nthesized techniques owing to the chemical and physical syntheses have their own disadvantages which consumed much energy and non-eco-friendly chemical reagents. The green synthesis overcomes the problems of physical and chemical syntheses techniques due to its use of less toxic chemical reagents, eco-friendly nature and one step method for green synthesis of ZnO nanoparticles. Green synthesis techniques generate the nanoparticles by using the plant extract. (Karthik et al., 2017). The green synthesis technique is the cleanest, biocompatible and eco-friendly method for large scale production of the nanoparticles using plant extract. The green synthesis nanoparticles are stable due to the core components in plant extract, such as poly-ol which acts as the chelating and capping agent for rapid biosynthesizing of nanoparticle and stabilizing the formation of the nanoparticles (Karthik et al., 2017).

After the green synthesised of the nanoparticles by using the plant extract, the prepared nanoparticles will effectively have coated with the hydroxyapatite as the support. The main reason of chosen hydroxyapatite as photocatalyst support owing to it can easily obtain from buffalo bone and environmental friendly. The hydroxyapatite is used as a support of nanoparticles due to the stability of the hydroxyapatite, strong adsorption capability, surface acidity/basicity and ion exchange ability (Fluidinova, 2018). It has been using as a porous support owing to the presence of the phosphate group which can stabilize the structure of active site. The ion exchange and adsorption ability properties of the hydroxyapatite promote the well-defined monomeric active species can be immobilized on photocatalyst surface based on the cation exchange capability and adsorption ability. The hydroxyapatite is used as support for semiconductor catalyst to perform the photocatalysis reaction and

explore its functional properties like UV protection, hydrophobicity, and excellent textural property.

1.3 Objective

This research paper aims to investigate the photocatalytic degradation of the rubber wastewater using green synthesised of ZnO photocatalyst with the hydroxyapatite (ZnO/Hap) as photocatalyst support under UVlight irradiation. The objective of this research contain:

1. To prepare and characterize the ZnO/Hap via the corn husk-mediated green synthesis.
2. To determine the performance of the prepared photocatalysts for glove wastewater degradation under UV light irradiation.
3. To determine the respective roles of active species using radicals scavenging chemicals.

1.4 Scope of study

This research concerned on the photocatalytic degradation of rubber wastewater utilizing green synthesized corn husk ZnO as photocatalyst. The primary stage of this study was to synthesize the corn husk ZnO photocatalyst and coupled with the natural synthesized HAp to enhance photocatalytic degradation. After that, the prepare catalyst will be characterized by using energy dispersive X-ray spectroscopy (EDX), Fourier transform Infrared spectroscopy (FTIR), x-ray diffraction (XRD), scanning electron microscope (SEM), UV-vis DRs, and particle size analyser (PSA). Additionally, main process parameters such as photocatalyst loading (0.5 g/L -1.5 g/L), , and initial wastewater concentration (10 ppm – 50 ppm) on the degradation of rubber wastewater will also be experimented.

CHAPTER 2

LITERATURE REVIEW

2.1 ZnO as Photocatalyst

2.1.1 Introduction of ZnO

ZnO is the molecular formula of zinc oxide. Zinc oxide is presented as a white powder and it is insoluble in water. It is extensively used as an additive in numerous products such as ceramics, rubber, lubricants, glasses, paints, plastics, adhesives, foods, pigments, batteries, ferrites and fire retardants. Zinc oxide is normally produced through the synthetic method routes in industry. Moreover, it also performs as the semiconductor in materials science. The zinc oxide is performing well as a semiconductor catalyst owing to its unique physical properties includes excellent transparency, high electron mobility, wide band gap, and strong room temperature luminescence. ZnO is type of the metal oxide semiconductors that is able to perform the photocatalyst. The metal oxide semiconductor catalyst that is used for photocatalysis is usually photostable and a non-toxic semiconductor that can absorb the ultraviolet or visible light. ZnO is also able to perform the photocatalysis either in micro and nanoscale which absorbs the ultraviolet light easily. The chemical reactions are to be induced by suitable irradiation taken place by contacting between their surfaces and fluid when applied in the photocatalysis reaction for water treatment. Besides, ZnO is able to perform the photocatalysis in different morphologies including nanoparticles, nanorods, nanowires, nanotubes, nanosheets

and nanoflowers. ZnO is chosen to use in photocatalysis reaction because of its unique physical properties. This is owing to their advantages such as low cost and good chemical stability (Akkari et al., 2018).

The photocatalyst with wide band gap energy is better than the low band gap which has higher free energy of photo generated charge carriers formed, low chemical and photochemical stability. ZnO is a semiconductor metal oxide that featuring both ionic and covalent behaviour. ZnO takes advantages of having the large band gap energy (3.3eV), an excitation binding energy (60 meV than TiO₂, 4meV), and can be synthesized easily in low temperature and different structure. In recent years, the semiconductor that is most probably used as the photocatalyst for degradation of emerging pollutants in wastewater is ZnO among others due to its extraordinary physical properties that can function well in heterogeneous photocatalysis. ZnO is a semiconductor catalyst with excellent physiochemical and wide band gap showing good optoelectronic, catalytic, excellent photochemical properties. ZnO is also a semiconductor with low cost, excellent UV shielding property, environmental stability and nontoxicity. (M.Akkari et al, 2018). ZnO is a II – IV binary compound featuring both ionic and covalent bonding. ZnO is an extensively known pyro and piezoelectric material owing to its central role that is employed by crystalline structure. ZnO can be exist in 3 different types of crystalline structure which are rocksalt, wurtzite, and cubic structure (Zinc Blende). Referring to the figure 2.1, there are three different type of crystalline structure of ZnO. The white and black spheres in the crystalline structure represent zinc and oxygen atom. The closed circle, open circle, and thick solid line indicate presence of cation, anion, and projection of two bonds, respectively.

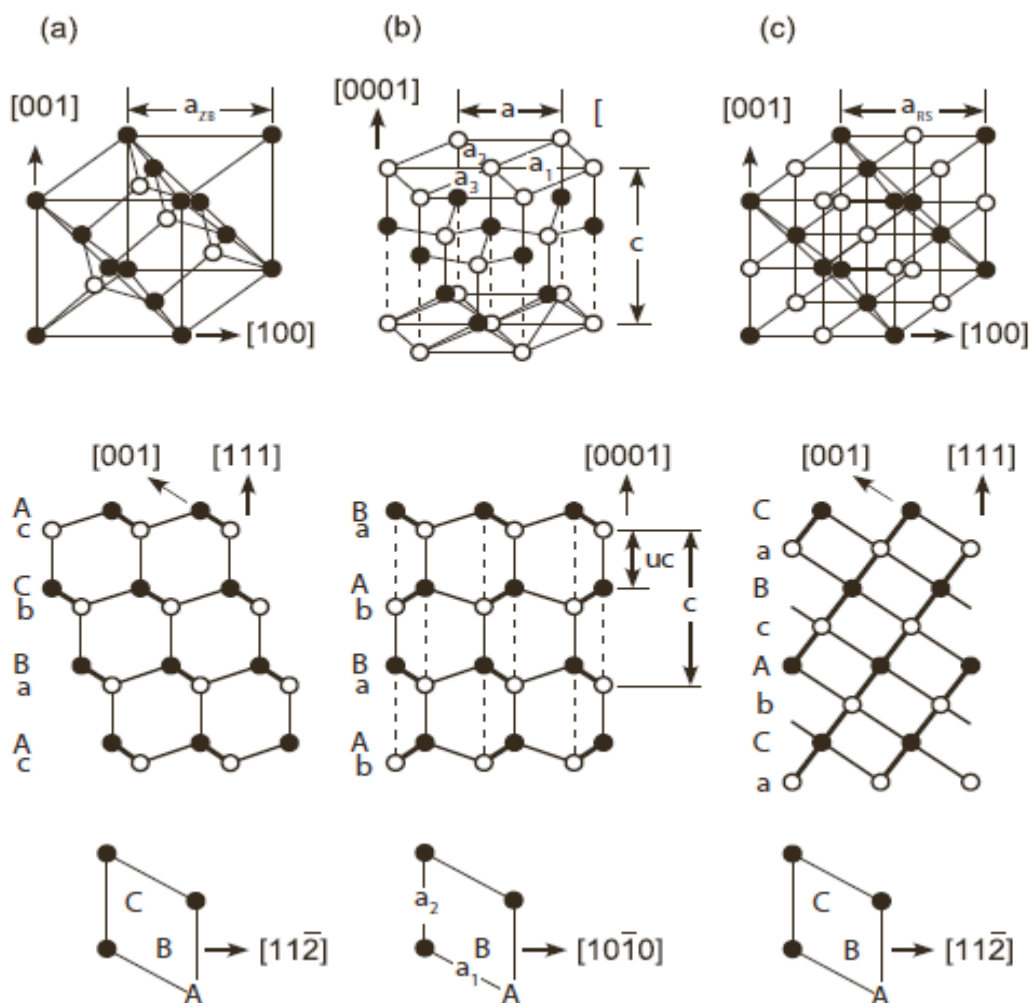


Figure 2.1: Three different atomic structure of ZnO (a) zincblende, (b) wurtzite and (c) rocksalt structures. (Hanada., 2009)

Zinc atom is tetrahedrally coordinated with four oxygen atom in wurtzite (WZ) crystal structure which is nearest atomic coordination as zinc blende (ZB) type structure. Crystal structure of the ZnO is usually hexagonal WZ structure owing to this crystal structure is thermodynamically stable at ambient condition. WZ hexagonal crystal lattice belongs to the space group $P6^3mc$ and it is described by two interconnecting sublattices of Zn^{2+} and O^{2-} , such as Zn ion is surrounded by a tetrahedral of O ions. The tetrahedral coordination of the ZnO WZ structure rises the polar symmetry along the hexagonal axis. Polarity of ZnO includes the properties of piezoelectricity and spontaneous polarization in crystal growth, etching and defect generation of ZnO WZ structure. The face terminated of the WZ ZnO includes the

polar and non-polar. The polar include the Zn terminated (0001) and O terminated (0001) faces (c-axis oriented) which poses their chemical and physical properties, while non polar (1120) (a-axis) and (1010) faces which both include an equal number of Zn and O atoms. However, ZB ZnO is stable only when it growth on cubic structures and rocksalt structure is a high pressure metastable phase forming at around 10 GPa.

Compare between the WZ crystal structure and ZB crystal structure, the difference between them is the former has AaBbAaBbAaBb stacking sequence along with the [0001] axis and the latter has the AaBbCcAaBbCc stacking sequence along the [111] axis. The A (a), B (b) and C(c) represent three kinds of cation and anion positions in the lattice sequence on the [0001] WZ planes and [111] ZB planes. Besides, the constant of triangular WZ lattice structure a and c have relation as $\frac{c}{a} = \sqrt{\frac{8}{3}} = 1.633$ while internal parameter $u = \frac{3}{8} = 0.375$, where uc corresponds to the length of the bonds parallel to [0001]. (Hanada., 2009).

Cation and anion atoms of the WZ structure is connected by dashed line along [0001] direction in figure above and attracted to each other by electrostatic force. The electronic interaction of the crystal structure make WZ-ZnO is more stable than ZB-ZnO owing to the ionicity of these compounds are bigger among the III-V and II-VI compound semiconductor. Therefore, length of dashed line of the wurtzite structure in the figure above tends to be shorter than ideal one. Owing to the previous can be complete mostly with angle deformation of the bond pairs so that it is easier to shorten the interlayer distances between A-b and B-a than to shorten A-a and B-b.

2.1.2 Semiconductors ZnO

The semiconductors are utilized to perform the heterogenous photocatalytic degradation reaction contains ZnO, TiO₂, WO₃, Fe₂O₃, CdS, ZnS, WS₂, ZrO₂, MoS₂ and SnO₂. Oxide based semiconductors are extensively used as heterogeneous photocatalyst owing to they are stable against photocorrosion. Semiconductors are used as heterogeneous photocatalyst and perform as electrodes.

The semiconductor catalysts have small band gap between the valance and conduction bands. Therefore, they have advantages to perform the photocatalytic reaction with the heterogeneous photocatalyst. The conduction band (CB) and valance band (VB) of the photocatalyst need to overcome oxidation and reduction potential in order to photo-oxidize an environmental contaminant. The semiconductor photocatalysts that are well positioned of CB and VB have priority to choose as semiconductor catalyst to perform the photocatalytic reaction. The efficient semiconductors have the oxidation potential of hydroxyl radical ($E^{\circ}\text{H}_2\text{O}\cdot\text{OH} = 2.8 \text{ V vs. NHE}$) and the reduction potential of superoxide radical ($E^{\circ}\text{O}_2\cdot\text{OH} = 0.28 \text{ V vs. NHE}$) positioned within the band gap. In the figure 2.3, the valance band, conduction band, and band gap energy was stated inside the table. The ZnO have the highest band gap energy.

Table 2.1: VB (valence band); CB (conduction band); and Eg (band gap energy). (Lam et al., 2012)

Semiconductors	VB (V vs NHE ± 0.1 V)	CB (V vs NHE ± 0.1 V)	Eg (ev)
ZnO	+3.0	-0.3	3.3
TiO₂	+3.1	-0.1	3.2
Fe₂O₃	+2.9	+0.6	2.3
SnO₂	+4.1	+0.3	3.8
ZnS	+1.4	-2.3	3.7
CdS	+2.1	-0.4	2.5

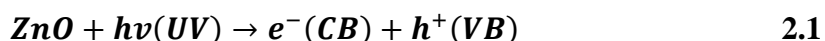
Furthermore, ZnO performs as a semiconductor catalyst for the photocatalytic reaction owing to ZnO has higher wide band gap energy than other semiconductors. The wide band gap energy are taking the advantages over the low band gap energy semiconductors owing to wide band gap energy semiconductors that has higher free energy of photo generated charge carries formed, low chemical and photochemical stability. TiO₂ is the semiconductor catalyst that is more preferred for the photocatalytic reaction owing to its 3.2eV band gap. However, ZnO has the advantages to perform as photocatalyst due to its advantages of direct band gap energy (3.2 ev) and an excitation binding energy (60 meV than TiO₂, 4 meV). According to the research and study, ZnO was performed well in photocatalytic reaction than other semiconductor catalysts showed in table 2.1. The semiconductors with small band gap are suffered from limit photoactivities, lacked reproducibility and less photoactivity. Besides, ZnO costs lower than other semiconductor catalysts and it is able to absorb over a large portion of the solar spectrum than other semiconductor catalyst. Therefore, ZnO takes the priority to utilize as semiconductor photocatalyst.

2.2 Principles of mechanism of ZnO photocatalyst

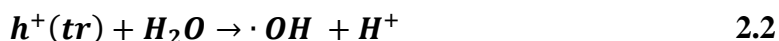
The efficient heterogeneous photocatalyst that perform well in photocatalytic reaction must have well positioned on conduction band (CB) and valance band (VB). Heterogeneous photocatalysis reaction will give a rise on the rate of thermodynamically and allow photocatalyst reaction to improve originating from the formation of new reaction pathways involving photogenerated species and reduction of the activation energy (Lam et al., 2012). Main four steps in mechanism of heterogeneous photocatalysis on the ZnO semiconductors catalyst surface includes charge carrier generation, trapping, recombination and phototcatalytic degradation of rubber chemical processes pollutants.

2.2.1 Mechanism of ZnO photocatalyst

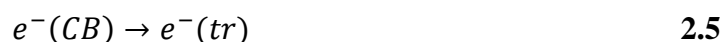
The direct band gap energy of the ZnO semiconductor photocatalyst is 3.3 eV. The e^- of the ZnO will be excited from valence band to conduction band when the UV light energy for irradiation of ZnO is equal or greater than its band gap energy. The photoexcited of the e^- from the VB to CB give the rise of formation h^+ in VB. The photoexcitation leaves behind a h^+ in the VB and formation of the e^- hole pair.



The h^+ that forms upon the photoexcitation is a strong oxidant that can direct oxidation with the absorbate pollutant or formation of hydroxyl radical OH reacting with the water or hydroxyl ion as electron donors.

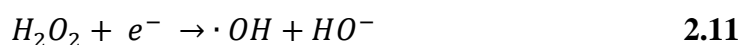
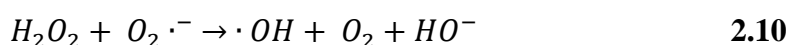
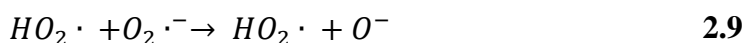


The charge carrier of the e^- hole pair will produce heat through the recombination themselves result in lower photocatalytic efficiency or trapped by recombination and excitation to the photocatalyst surface (Lam et al., 2012).



When the trapped charge (tr) particles is under aqueous environment, the photocatalyst would be in electrostatic equilibrium. Therefore, the photoexcitation of the e^- hole pair to the surface is equal. Besides, it is important for the trapped $e^-(CB)$ scavenged by an e^- acceptor to maintain the charge equilibrium and inhibit its recombination with the h^+ hole trapped in valence band. The oxygen molecule is efficient e^- acceptor where they undergo the reduction with e^- to generate reactive superoxide radical anions (O_2^-). On the other hand, the $\cdot OH$ radicals can be

generated through other oxidizing species includes hydroperoxyl radicals ($HO_2 \cdot$) and hydrogen peroxides. Oxygen is the most common to employ as electron scavenger owing to it is cost effective as it is simple and cheap to spurge solution with air. The series of further reactions that can occur to form the $\cdot OH$ radical are shown in equation below (Lam et al., 2012).



The $\cdot OH$ radical generated is a powerful oxidizer that can convert the organic contaminants inside the wastewater into less harmful product such as CO_2 and H_2O . Table 2.1 below shows some organic pollutants degraded by ZnO photocatalyst.

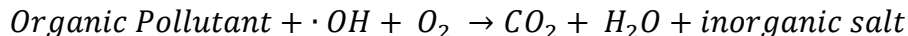


Table 2.2: List of Oranic pollutants degradable by ZnO photocatalyst

CLASS	EXAMPLES	REFERENCE
Halophenols	4-nitrophenol, Chlorophenol	Rajamanickham and Shanthi (2016); Hariharan (2006)
Dyes	Rhodamine B, Methylene Blue, Arridine Orange	Amani and Ashrafi (2015)
Phenolic compound	Phenol, p-Cresol	Sin et al. (2013); Abdollahi et al. (2011)
Surfactants	Polyethoxylate	Giahi, Ghanbari and Issazadeh (2013)

Aromatics	Aniline, Benzoquinone	Pirsaheb et al. (2017); Abdollahi et al. (2012)
Alcohols	N-butanol	Kirchnerova et al. (2005)
Aromatic Carboxylic acid	Benzoic acid	Benhebal et al. (2013)

2.3 Green Synthesized of ZnO Nanomaterials

Nanoparticles are extensively integrated by different methods which enhance the chemical reactivity, thermal conductivity, non-linear optical performance and chemical steadiness due to its larger surface area to volume ratio. There are different synthesis methods that are available for synthesizing the nanoparticle such as chemical, physical and green synthesis method. The physical method is applying the physical force to generate the large, stable and well defined nanostructure. However, the physical method is utilized of high cost equipment, high pressure and temperature, requires of large area for setting up the machine. Chemical and physical synthesis technique involve the use of capping and stabilizing agent as well. On the other hand, the chemical and physical synthesis method involve the use of toxic chemical for synthesizing the nanoparticle. Therefore, the nanoparticles that synthesized from both physical and chemical method may prove hazardous in their application. (Spitia et al., 2011)

With the sustainable development of the synthesis method, the green synthesis method is preferring to apply owing to these methods are environment friendly, cost effective and biocompatible methods for synthesis the nanoparticle. The green synthesized nanoparticle can be synthesized through plant, bacteria, fungi, algae etc. The green synthesis method allows the large scale production of ZnO nanoparticles with less impurities and reduces the use of costly equipment and toxic chemical for synthesizing. Besides, the nanoparticle that is synthesized through the green method also perform with more catalyst activity. The green synthesis method

of nanoparticles through plant extract that is formed at ambient temperature, neutral pH, low cost and environmental friendly. Among the green synthesis methods through biological alternatives, the plant and plant extracts are better choices for synthesizing the nanoparticles owing to plant extracts method require low maintenance and cost efficient. The green synthesized of nanoparticles through different plant extract will give different natures of the nanoparticles. The plant extract from different sources may contain different amounts and concentrations of organic reducing agents.

Green synthesized method through the plant extract are presenting superiority over both chemical and physical synthesized method. The photocatalyst that synthesized from the plant extract act as both reducing and stabilizing agent due to the supplement inside the plant. The nanoparticles that synthesized through the chemical method cause the rise of adverse effect on the ecology. Therefore, the plant extract synthesized method is preferred by the researcher owing to its salubrious nature towards the environment. From the point of view of the industry, the plant extract synthesized method produces much lesser toxic waste (Lakshmi at al, 2017).

The chemical method requires the costly equipment and expensive chemical to synthesize the nanoparticles. However, the plant extract method is provided with the low maintenance cost and the waste disposal requires less effort among other factors. The plant extract method is preferring to use than the biological method owing to the maintenance system of all plant synthesized method is much lesser than a culture bacterium which need a myriad of phenomena to be taken care of The research from recent studies are also shown that the therapeutic effects of nanoparticles that synthesized from the plant extract eliminate the need of artificially generation of a drug for that particular ailment.

The synthesized method for generating the ZnO photocatalyst are continuously developed by the researcher. The synthesized method for ZnO nanoparticles without using of the toxic chemical and environmental friendly method is green synthesized method. The ZnO nanoparticles that apply for photocatalysis reaction synthesized by the green method will show with no hazardous to the

environment. Since the green synthesized method will reduce the toxicity so that the toxicity of nanoparticles or toxicity of reaction environment also will decrease. Therefore, the green synthesized ZnO nanoparticles are suitable for different applications such as skin care and food industry. The green synthesized method allows the large scale production of ZnO nanoparticles with zero impurities and reduce the use of costly equipment and toxic chemical for synthesizing (Elumalaia et al., 2016).

Table 2.3: The green synthesized of ZnO through the different leaf and fruit extract

Plant Name	Part of plant taken as extract	Size(nm)	Structure	References
Aloe Vera	Leaf Extract	XRD – 8-20	Spherical, Hexagonal	Oval, (Ali et al.,2016)
Black Nighthshade	Leaf Extract	XRD and FE-SEM – 20-30, 29.79 TEM - 25-65	Wurtzite, quasi-spherical	hexagonal, (Ramesh et al., 2015)
Kapurli	Leaf Extract	XRD - 56.24 FE-SEM - 20-40 TEM – 30-40	Hexagonal quasi-spherical	Wurtzite, (Anbuvarnan et al., 2015)
Drumstick tree	Leaf Extract	XRD – 24 FE-SEM – 16-20	Spherical and nano sized shape	granular (Elumalai et al., 2015)

Water hyacinth	Leaf extract	SEM and TEM – 32-36 XRD – 32	Spherical	(Vanathi et al., 2014)
Mexican Mint	Leaf extract	SEM - 50-180	Rod shape nanoparticle with agglomerates	(Fu et al., 2015)
Red Rubin Basil	Leaf extract	EDS – 50 XRD – 14.28	Hexagonal WZ	(Abdul et al., 2014)
Stone Breaker, Bhuiamla	Leaf extract	SEM and XRD – 25.61	Hexagonal wz structure, quasi spherical	(Anbuammam et al., 2015)

Table 2.4: The green Synthesized of ZnO through the fruit extract.

Plant Name	Part of plant taken as extract	Size (nm)	Structure	
Dog Rose	Fruit Extract	XRD - 13.3 (CH), 113 (MI) DLS - 25-204 (CH), 21-243 (MI)	Spherical	(Jafarirad et al., 2016)
Rambutan	Fruit peels	XRD - 20.95	Needle-shaped forming agglomerates	(Yuvakkumar et al., 2014)
Coconut	Coconut water	TEM - 20-80 XRD - 21.2	Spherical and predominantly hexagonal without any agglomeration	(Krupa et al., 2016)

2.4 ZnO supported on hydroxyapatite (ZnO/Hap)

ZnO is an important functional oxide with 3.3 eV band gap are very suitable as a semiconductor photocatalyst owing to its outstanding photocatalytic activity/degradation, low cost and environmental friendly as compared with other metal oxides. Generally, 3D hierarchical ZnO structures assembled can deliver more reaction interface than other nanostructure. The study from Wang et al proved that the three dimensional ZnO taking better photocatalytic reaction for organic pollutants degradation owing to their high surface area compared to ZnO powder and ZnO nanocone. Nevertheless, the fast recombination of e^- hole pairs of ZnO unavoidably hindered the outward diffusion of the charge carrier. Therefore, it will decelerate the redox reactions at the solid-liquid interface. Therefore, few studies have reported that decorating of ZnO with photocatalyst support was an advantageous method to enhance the photocatalysis of ZnO.

Hydroxyapatite is emerged to use as a support of nanoparticles due to the stability of the hydroxyapatite, strong adsorption capability, surface acidity/basicity, and ion exchange ability (Fluidinova., 2018). Besides that, one of the main reason of chosen hydroxyapatite as photocatalyst support owing to it can easily obtain from buffalo bone and environmental friendly. It has been using as a porous support owing to the presence of the phosphate group which can stabilize the structure of active site. The ion exchange and adsorption ability properties of the hydroxyapatite promote the well-defined monomeric active species can be immobilized on their surface based on the cation exchange ability and adsorption capacity. The design of the heterogeneous catalyst based on the hydroxyapatite as a support of catalyst is emerged and also exhibits the well performance in the reaction owing to its physical and chemical properties.

High performance of the heterogeneous catalysts can be designed by employing the hydroxyapatite as a microligand for catalytically active centres. The heterogeneous catalyst generated as nanocluster on the hydroxyapatite surface has proven as a catalytically active species. Non porous structure of the hydroxyapatite takes the advantage to solve the problem towards mass transfer limitation. Furthermore, the weak acid base properties also minimize side reactions induced by

the support itself. By varying calcium and phosphate ratio, phosphate group of hydroxyapatite (HAp) is allowed to control the acid base properties.

The heterogeneous photocatalyst that is supported by the HAP, $\text{Ca}_{10}(\text{PO}_4)_6(\text{OH})_2$, has been studied that it exhibits a greater photocatalytic activity compared with either photocatalyst itself or hydroxyapatite. Refer to Hu et al (2018), the hydroxyapatite itself has no activity for photocatalytic degradation owing to it is too wide band gap which is 4.85 eV which exceeds the limitation of the UV lamp. The optical band gap energies for hydroxyapatite varies greatly and found with 4.85 eV of band gap which is close to the reported one. Density Functional Theory calculation proves that an O vacancy from the OH group resulted generating high band gap energy of more than 5 eV. Band gap energy of the hydroxyapatite (4.8 eV) may include intrinsic OH vacancies in its structure. The TiO_2/HAP in Hu et al (2018) study are found to have 3.4 eV which is larger than the band gap of individual TiO_2 (3.22 eV). Since the band gap energy of the ZnO are 3.4 eV, coupling ZnO photocatalyst with the hydroxyapatite are estimated to have higher band gap energy than 3.4 eV. The wide band gap energy photocatalyst has been proven that more sensitive under experiment UV region (Bystrov et al., 2016).

Activation energy of the photocatalyst doped with hydroxyapatite are found lower than the individual photocatalyst without doped with hydroxyapatite. Photocatalytic reaction is not involved heating and usually operate at ambient temperature attribute to the photonic activation during photocatalysis reaction. Activation energy of the hydroxyapatite doped photocatalyst which is lower indicates that it is more active for the photocatalytic degradation. On the other hand, the insertion of the photocatalyst such as ZnO into the HAp lattice increase the light absorption in the UV with the adsorption being stronger for higher photocatalyst ions concentration (Buazar et al, 2014). This is owing to strong absorption properties of the hydroxyapatite. Besides, the UV irradiation of the photocatalytic degradation leads to create an O vacancy in the hydroxyapatite lattice. The hydroxyapatite vacancy leads the transfer of an electron to the atmospheric oxygen which generate the charged O_2^- species. The O_2^- species will react with the liquid/ gaseous molecules and degrade them. Refer to the study from Buazar et al, 2014 the degradation efficiency of the ZnO/Hap nanocomposites used for degrade the 2-

mercapto-benzole (MBO) achieved 99% efficiency after 2 hours owing to its larger specific surface area and high generation of active $O_2 \cdot^-$ and $\cdot OH$ species.

Table 2.5: Hydroxyapatite as a Catalyst Support

Photocatalyst/ Hydroxyapatite	Eg, Band Gap Energy	Application	References
ZnO/ Ca ₅ (PO ₄) ₃ OH		Degradation of 2-mercapto-benzole (MBO)	(Buazar et al., 2014)
TiO ₂ /Ca ₅ (PO ₄) ₃ OH	3.3 ev	Reduce the toxicity to half	(Fabrício., 2018)
Fe ₃ O ₄ / Ca ₅ (PO ₄) ₃ OH		degradation of the insecticide diazinon under UV irradiation	(Yang et al., 2010)
TiO ₂ /Ca ₅ (PO ₄) ₃ OH	3.3 ev	photo-degradation of MB	(Guo et al., 2017)
Ni/ Ca ₅ (PO ₄) ₃ OH, Ce/ Ca ₅ (PO ₄) ₃ OH, Cu/ Ca ₅ (PO ₄) ₃ OH		Steam reforming reaction of glycerol.	(Hakim et al., 2016)
Pa/ Ca ₅ (PO ₄) ₃ OH		Selective Oxidation of Alcohols by Use of Molecular Oxygen	(Mori et al., 2004)
Au/ Ca ₅ (PO ₄) ₃ OH Ru/ Ca ₅ (PO ₄) ₃ OH		water gas shift reaction	(Venugopal., 2003)

2.5 Review on the glove wastewater

Glove industry is one of the manufacturing industries that generates large amount of wastewater and pollutes the water sources owing the rubber industries dominates large number of manufacturing industries in Malaysia. The effluent of the rubber industry consists of large amount of water, uses chemical and other utilities from the manufacturing that will kill aquatic life. Natural rubbers are extensively used in glove manufacturing and products. It can be derived from the milky colloidal suspension or latex and synthesized from chemical isoprene. There are some chemicals that are used for manufacturing the natural rubber such as organic and inorganic acid and ammonia in various quantities are used. The operating procedure of a glove production requires dipping process for cleaning the gloves former which needs some alkaline and acid are hazardous. Therefore, the wastewater from the glove or rubber industry without treated is classified as hazardous and it will bring harmful effect to the aquatic life. The wash water, unreacted chemicals and settleable solid from the processing of glove contain high biochemical oxygen demand (BOD), chemical oxygen demand (COD), nitrogen, pH, total suspended solid (TSS) and ammonia. Table 2.5 shown that characteristic of the glove wastewater is classified as acidic water in the range of pH 3.7-5.5 and it also contained large amount of suspended solids, total nitrogen (200-1800) and sulphate content.

Table 2.6: The characteristic of glove wastewater.

Parameter	Range
pH	3.7-5.5
BOD	1500-7000
COD	3500-14000
TSS	200-700
Total nitrogen	200-1800
Sulphate	500-2000

The disposal of these glove processes effluent into the water sources will cause serious depletion of dissolved oxygen. Therefore, the effluent will affect the environment that supports the aquatic life. The glove manufacturing wastewater consists of mainly nitrogenous compound. The presence of the nitrogenous compound inside the effluent owing to the ammonia are utilized for the preservation of the latex. Algal will emerge to growth when there is high level of NH_4^+ and other plant nutrient resulting in the eutrophication of water bodies. Therefore, it needs some acts to regulate the manufacturing industries to discharge their waste and follow the laws and regulation. Besides, sulphuric acid is also applied in the coagulation of the skim latex during the processing and resulting in composition of high level sulphate in the rubber effluent.

Hydrogen sulphide will cause the malodour problems and inhibit digestion process which give lower organics pollutants removal efficiency. Odours can be detected even at low concentration and make water unpalatable for several hundred miles downstream from the processing plant. According to the Malaysia Environmental Law, Environment Quality Act 1974 and Malaysia Environmental Quality (Sewage and Industrial Effluent) Regulations, 1979, 1999, 2000 has generated some limitations for the effluent that discharges (Elaw., 2018). The table 2.6 is the parameter limits of effluent of standards a and b that regulated by the Malaysia Environmental Law. Besides that, few study also carried out the analysis of the rubber and glove wastewater characteristic that shown in table 2.7. The studied from the Loh (2001), observed that the high BOD level of the glove wastewater is 85-1035 mg/L and COD is 300 mg/L-4360 mg/L. The glove wastewater also contained large amount of total suspended solid up to 1305 mg/L.

Table 2.7: Limits of Effluent of Standards A and B (Elaw., 2018)

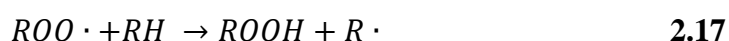
Parameter	Unit	Standard A	Standard B
Temperature	°C	40	40
pH		6.0-9.0	5.5-9.0
BOD at 20 °C	ppm	20	50
COD	ppm	50	100
TSS	ppm	50	100
Mercury level	ppm	0.005	0.05
Cadmium level	ppm	0.01	0.02
Lead	ppm	0.10	0.5
Copper	ppm	0.20	1.0
Nickel, Tin , Manganese	ppm	0.20	1.0
Zinc	ppm	1.0	1.0
Boron	ppm	1.0	4.0
Iron (Fe)	ppm	1.0	5.0
Free Chlorine	ppm	1.0	2.0
Sulphide	ppm	0.50	0.50
Oil and Grease	ppm	Not detectable	10
Phenol	ppm	0.001	1.0
Cyanide	ppm	0.05	0.10
Arsenic	ppm	0.05	0.10
Chromium	ppm	0.2	1.0
Trivalent	ppm	0.2	1.0

Table 2.8: The research paper on the characteristic of rubber wastewater

Rubber Industry	Hazardous	Wastewater Characteristic	References
Rubber Glove Processing - Plant		BOD 85-1035 mg/L TSS 32 mg/L – 1305 mg/L COD 300 mg/L – 4360 mg/L	(Loh., 2001)
Natural rubber processing sector	(NR) Ammonia	pH 5.7 ± 0.30 , TDS (mg / l) 2240 ± 3.4 , TSS (mg / l) 3512 ± 4.8 , TS (mg / l) 5752 , Ammonia (mg / l) 94 ± 3.0 , Phosphate (mg / l) 48 ± 2.0 , BOD (mg / l) 1340 ± 2.0 , COD (mg / l) 2834 ± 1.9	(Pillai et al., 2014)

2.6 Photocatalyst Degradation of the Rubber Wastewater

Although the biodegradation is common to use for treat wastewater, however, biodegradation by using bacteria is sensitive to the level of toxicity and environmental condition in the ground. The condition for the biodegradation must be conducive to microbial activity and these degradation is required to consider temperature and pH. If the process is not under controlled or monitored, the organic contaminants may not be fully broken down. Therefore, the toxic by product could be more volatile than initial contamination. With the sustainable development of the degradation method, the oxidation degradation methods are employed for destruction of organic contaminants in wastewater. Advanced oxidation process (AOPs) were first proposed in 1980s used for potable water treatment which involves two oxidation stages. The process is first in formation of highly reactive hydroxyl radicals as strong oxidant by converting hydrogen peroxide and followed by reaction of oxidants with organic matter in water. The organic matter will undergo mineralization and become less harmful inorganic components (water, carbon dioxide and salts) (Mazille., 2008). Ozone and hydrogen peroxide are often used to remove hazardous water pollutants owing to its high oxidation potential. High reactive hydroxyl radical ($\text{OH}\cdot$) produced when combination of the ozonation and UV radiation and making it a more effective advanced oxidation process. Hydrogen peroxide makes the pollutant more susceptible to ozone attack in advanced oxidation process (AOPs) whereas UV-light provides energy to break chemical bonds. Equation below shows degradation mechanism of organic contaminants by OH radical. (Munther., 2010).



Advanced oxidation processes (AOPs) are performed by different external energy sources which can be categorized into photochemical or not photochemical. Photochemical utilizes the solar light and UV light which is known as light driven AOP method. The photochemical is more common to use owing availability of sunlight in places where high water scarcity is detected. Table below shows the example of photochemical and non-photochemical AOPs (Lam et al., 2012).

Table 2.9: Examples of non-photochemical AOPS (Lam et al., 2012)

Non-photochemical AOP	Photochemical AOP
Ozone (O₃)	Photolysis (UV+ H ₂ O ₂)
Fenton (Fe²⁺ + H₂O₂)	Photocatalysis(Light + Catalyst)
Electrolysis (Electrodes + Current)	Photo-Fenton (Solar Light + Fenton)
Sonolysis (Ultrasounds)	

AOPs can be categorized into different types of methods that can be used to treat the wastewater including the homogenous and heterogeneous photocatalytic processes. Homogenous AOPs are single phase process and heterogeneous AOPs are utilizing catalyst support on semiconductors such as ZnO, TiO₂ and WO₃. Homogenous process involves chemical reaction through interaction between reagents and target compound. Hence, Heterogeneous AOPs involve adsorption of reactant and desorption of product at the surface of catalyst. Therefore, pore structure and surface characteristic of catalyst may affect the reaction effectiveness.

Heterogeneous photocatalysis is the process focus in this study. The photocatalyst reaction follows free radical mechanism initiated through interaction between a catalyst and photons with certain energy level. In this study, the photocatalyst that is chosen to used is ZnO owing to its extraordinary physical properties that function well in heterogeneous photocatalysis reaction. Heterogeneous photocatalysis has limited application in drinking or wastewater

treatment owing to ozonation. However, heterogeneous photocatalysis still receive enormous amount of research interest owing to the extraordinary advantages of the process. The generation of sufficient $\cdot\text{OH}$ radical by using the combination of natural sunlight with appropriate catalyst is relatively low cost.

2.7 Effect of operating parameter

2.7.1 Effect of Photocatalyst Loading

The photocatalyst loading also one of the important factors that will affect the degradation efficiency of the photocatalytic reaction. The decomposition efficiency of the organic pollutants was found to be increase with the increase of the photocatalyst loading. This is owing to the increased of the effective surface of the catalyst area and able to absorb large amount of light. In fact, there are more active site of the ZnO catalyst for carrying out the photocatalytic reaction by increasing the quantity if active surface area of catalyst. Hence, there are more catalyst exposed to the light and increase the amount of photon absorption. When the photocatalytic reaction increases, the number of active radical generated also increases. Therefore, degradation of the pollutants increases and enhance the degradation efficiency to increase as well.

If photocatalyst loading overloaded, the degradation efficiency can be decreased owing to the interception of the light by suspension. The turbidity of the suspension resulting in the reduction of the effective photoactivated volume of suspension. Therefore, light penetration decreases with the amount of photon absorbed also decreases. As a result, the number of the active sites of the ZnO nanocatalyst decreases so that the degradation efficiency also decreases. With these two phenomena clashing with each other, it is important to obtain the optimum amount of photocatalyst to prevent unnecessary excess catalyst as well as to ensure maximum photon absorption that can efficient photocatalytic degradation of pollutants (Lam et al., 2012; Lee et al., 2016).

Research from the Buazar et al. (2014) studied the effect of catalyst loading with the initial concentration 0.1 g/L on the photodegradation of 2-mercapto-benzoxazole(MBO) pollutant using ZnO/Hap photocatalyst. The optimum photocatalyst loading in their study is 0.05 g/L with given degradation efficiency of 99%. Uti, Laouedj and Ahmed (2011) studied the effect of catalyst loading with the

initial dye concentration (20 mg/L) on the photodegradation Congo Red Dye pollutant using ZnO photocatalyst. The optimum amount obtained from this study is the 0.25 to 0.5 g/L of photocatalyst loading with given the degradation efficiency increased from 68.73 % to 95.02 %. On the other hand, the overload photocatalyst loading in this study by increasing the amount to more than 0.5 g/L showed a decrease in degradation efficiency of the dye. Another study is the Methyl Orange dye as model pollutant from Kaur, Bansal and Sigal et al (2013). This research examines the photocatalyst activities using ZnO nanocatalyst at different catalyst dosage loading from 0.25 to 2.0 g/L. When amount of catalyst increased from 0.25 to 2.0 g/L, degradation efficiency increased from 58.9% to 95.3 %. As a result, obtaining the optimum amount of the photocatalyst loading may increase the degradation efficiency of the photocatalytic degradation.

Table 2.10: Effect of semiconductor catalyst loading on the photocatalysis experiment.

Targeted Pollutant	Semiconductor Catalyst	Range of photocatalyst concentration (g/L)	of Optimum catalyst concentration (g/L)	Degradation / Mineralization Efficiency	References
2-mercapto-benzoxazole(MBO)	ZnO/Hap	0.001-02 g/L	0.05	99%	(Krishnakumar & Swaminathan., 2011)
Textile Effluent	ZnO-TiO ₂ -HAp		5	99.99%	(Mordirshala et al., 2011)
Acid Yellow 36	ZnO	0.25-0.15	1.0	90%	(Khezrianjoo & Revanasiddappa., 2013)
Brilliant Golden Yellow	ZnO	0.1-3.0	1.0	99%	(Ashan Habib et al., 2012)
Brilliant Red	ZnO	0.1-0.7	0.4	100%	(Jayamadhava et al., 2014)
Mordant Black 11	ZnO	0.1-0.4	0.4	99%	(Miao et al., 2014)
Reactive Black 5	ZnO	0.25-1.5	1.25	100%	(Kansal, Kaur & Singh., 2009)
Reactive Orange 4	ZnO	0.75-1.5	1.0	100%	(Kansal, Kaur & Singh., 2009)

CHAPTER 3

METHODOLOGY

3.1 Flowchart of the Work

This study comprised of several experiment steps. Figure 3.1 summarize overall steps that were conducted in this study:

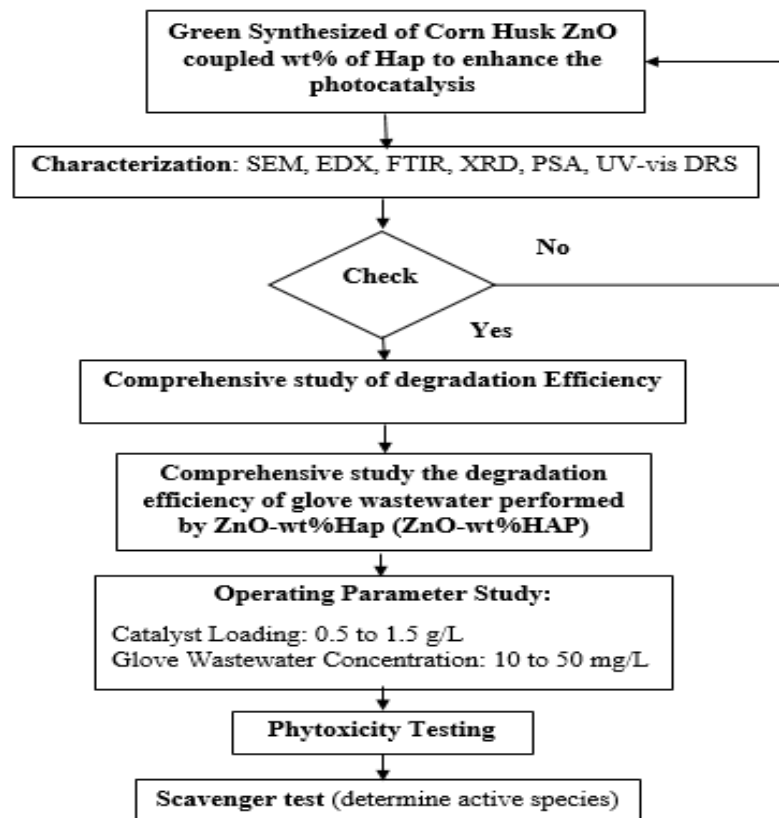


Figure 3.1: General Flow Chart of the work

3.2 Material and Chemicals

Table 3.1: List of chemicals and materials utilized in this study

Chemical/ Material	Purity	Supplier	Application
Ethanol (C₂H₆O)	99.8%	ChemSoln	Synthesized of photocatalyst Active Species Study
Distilled Water		Gainson Advanced Technology	Synthesized of photocatalyst pH adjustor
Sodium Hydroxide (NaOH)	≥96%	Uni-Chem Reagents	pH adjust
Potassium Iodide (KI)	99.995%	Merek Sdn Bhd	Active Species analysis
Sulphuric acid (H₂SO₄)	95-97 %	QRec	pH adjustment
Zinc(II) Nitrate Hexahydrate (Zn(NO₃)₂.6H₂O)	98%	Sigma-Alrich	Zinc precursor

3.3 Photocatalytic Degradation Experiment Setup

A batch reaction system was used in laboratory experiment setup. The photocatalysis were conducted in a 250 mL beaker under the presence of light source. Light source for this experiment was UVc lamp irradiated on the wastewater sample surface. The wavelength of fluorescent lamp ranged from UV to visible light. It was placed 12 cm above the surface of the wastewater sample. All the experiment setups including the UV lamp, beaker, and stirrer were located inside an acrylic black box to ensure that there was no stray light can enter into the photolysis system. Air pump using in this experiment was provided by the Sobo was utilized to introduce the air into the sample through the experiment. The flow meter supplied by Dwyer were utilized to control the amount of air flowed. A chilling blower fan supplied by Toyo was utilized for chilling purpose. The schematic diagram of this photocatalytic degradation laboratory setup is shown in Figure 3.2.

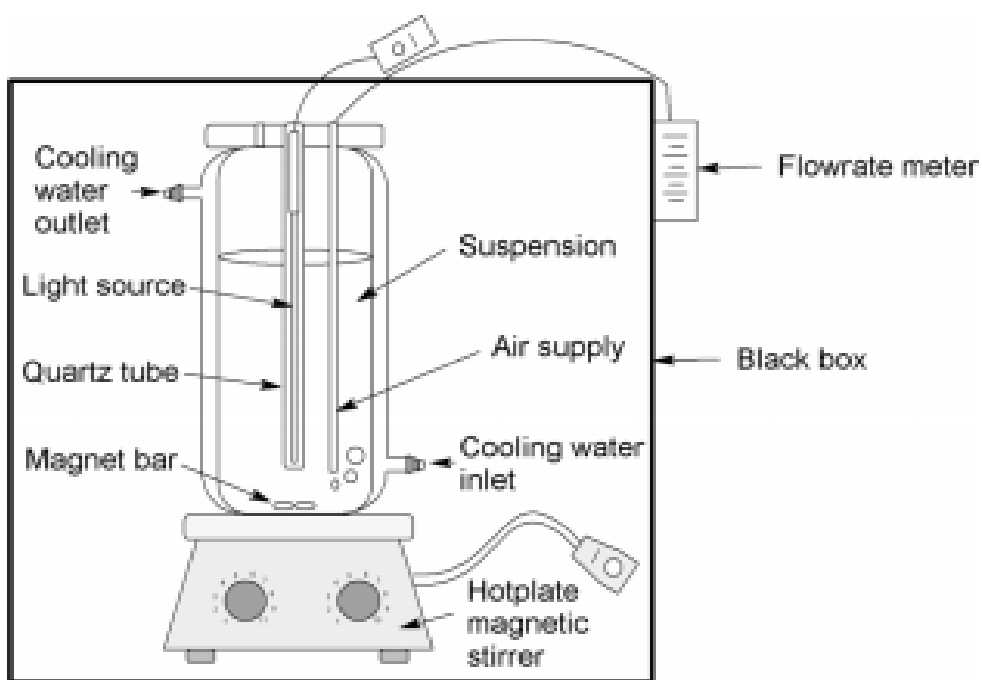


Figure 3.2. Schematic Diagram of the Photocatalysis System under UV-c irradiation. (Chin et al., 2018)

3.4 Preparation of ZnO-supported Hap photocatalyst

3.4.1 Preparation of Corn Husk Extracts

The plant wastes of corn husk, used for this experiment were collected from local markets in Kampar, Perak, Malaysia. Plant wastes such as corn husk were washed separately with tap water to remove dust particles and dried in oven at 40-50 °C for 2 days. After that, the dried plant wastes were blended using a commercial blender (CJX-SP450, Selangor, Malaysia). The blended plant waste was measured and poured into the thimble before put inside the soxhlet extractor. Each blended plant wastes was extracted separately in a soxhlet extractor using 50% ethanol aqueous solution. The extraction is carried out 2 hours and heating at 100°C to extract the blended plant waste by using the heating mental and reflux condenser. The extracts were dried over a water bath at 90 °C for 2hr to obtain crude extracts, filtered and placed into individual air-tight bottle before stored in a refrigerator at 4 °C.

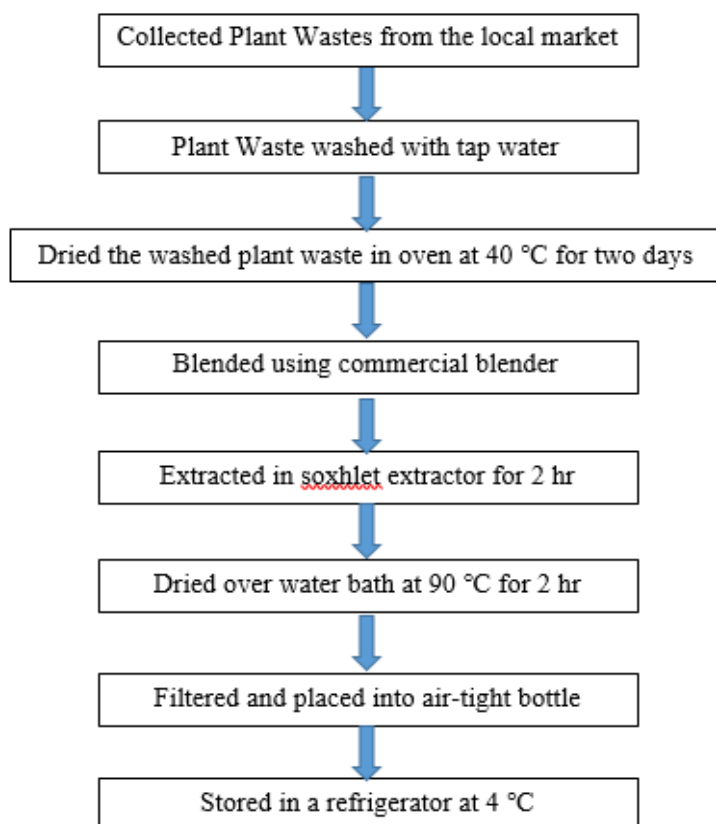


Figure 3.3: Flow Chart of preparation of green extracts

3.4.2 Preparation of Green synthesized corn husk ZnO

Firstly, 0.1 M of $\text{Zn}(\text{NO}_3)_2 \cdot 6\text{H}_2\text{O}$ was prepared with 60 mL of water. Then, 20 mL of plant waste extract taken out from the refrigerator was added into the mixture and continuously stirred afterwards. Then, the mixture solution was adjusted to approximate pH 12 with addition of 5M of NaOH. The resultant mixture was stirred continuously by using the magnetic stirrer at 80 °C for 4 hours (Sohrabnezhad and Seifi., 2016). The pale white precipitate was obtained through centrifugation and washed with ethanol and water before filtered down to a filter paper. The filter paper that contains the white precipitate will then be allowed to dry in the oven at 90 °C. After drying, the dry product was placed in the muffle furnace at 400 °C for 1 h. The calcined product was allowed to cool in a desiccator. The product was then ready (Sohrabnezhad and Seifi., 2016).

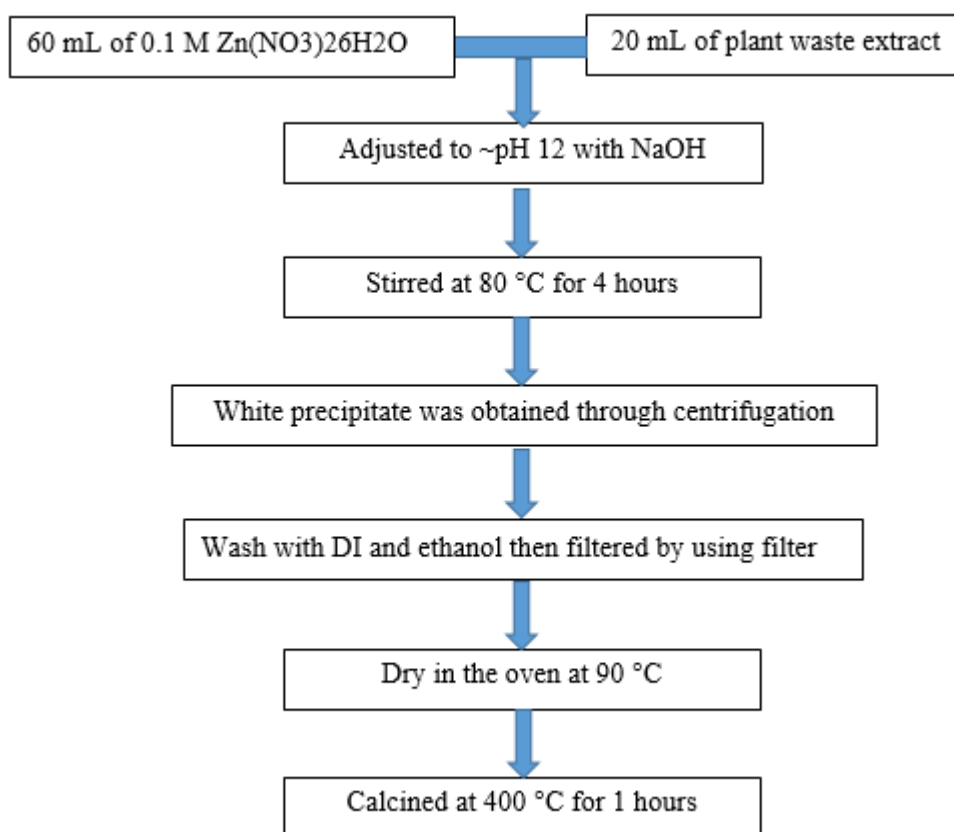


Figure 3.4: Flow Chart of preparation of ZnO

3.4.3 Preparation of Bone derived photocatalyst (Hydroxyapatite)

The bovine bone (femur) waste was collected from a local butchery in Kampar, Perak, Malaysia. The adhering soft tissues of the bovine bone were removed manually with a stiletto knife and washed under tap water. The bones were then sawed into smaller pieces with a hacksaw and boiled for 3 h to facilitate the removal of any organic substance on the bone. An alkali-heat treatment was then conducted to de-fat and de-proteinase the bone. In the alkali-heat treatment, bones were treated with a 20 wt% sodium hydroxide aqueous solution and heated in water bath at 80 °C for 10 h. The treated bones were later dried at 80 °C for 3 h and grinded using RETSCH Ultra Centrifugal Mill ZM 200. The powdered bone was sieved with a 250 µm mesh size and its product was calcined in a muffle furnace at 550 °C for 2 h.

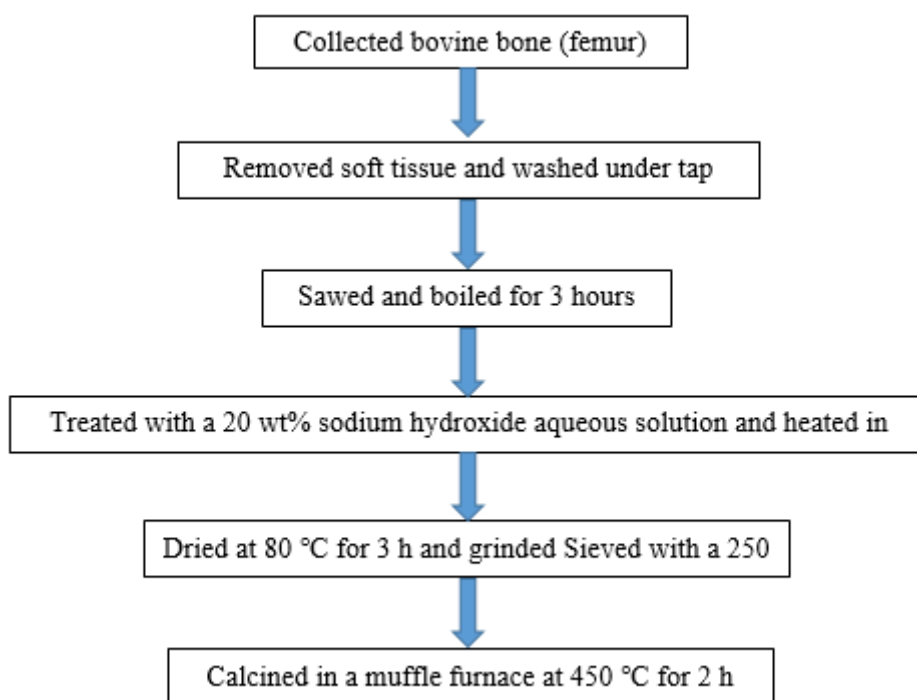


Figure 3.5: Flow chart preparation of Bone derived photocatalyst (Hydroxyapatite)

3.4.4 Preparation of Green Synthesized ZnO/HAp

Firstly, the ZnO/HAp composites were prepared by dispersing 1.0 g of the green synthesized prepared ZnO and different amounts of HAp in deionized water. The mixture was ultrasonicated for 30 min and mechanical mixed for 17 hours under room temperature. Then, the ZnO/HAp composites were collected by centrifugation, dried at 65 °C for 12 hours and calcined at 450 °C for 2 hours (Chin et al., 2018). The synthetic procedure for preparing the ZnO/HAp composites is schematically depicted in Figure 3.6. The obtained samples with 20, 30, 40 and 50 wt% HAp nanoparticles were denoted as ZnO-20%HAp, ZnO-30%HAp and ZnO-40%HAp, respectively (Chin et al., 2018).

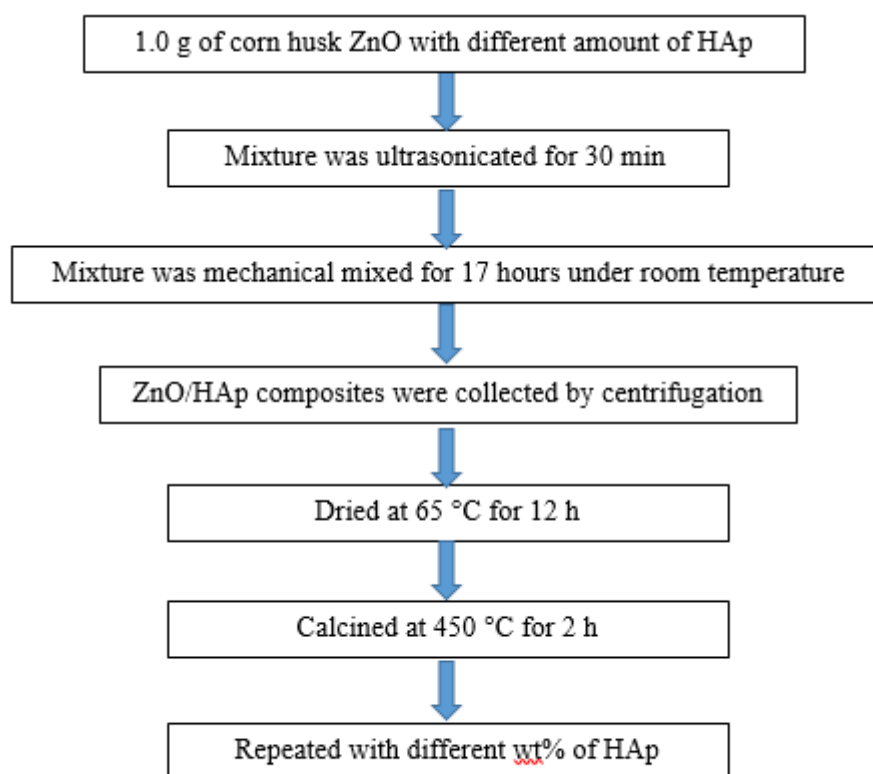


Figure 3.6 Flow Chart of preparation of Green Synthesized ZnO/HAp

3.5 Characterization of Photocatalyst

3.5.1 X-Ray Diffraction (XRD)

The crystal phase of ZnO/HAp photocatalyst was analysed by X-Ray Diffraction machine (XRD-600) supplied by Shimadzu. The XRD data were scanned at 2θ from 20° to 70° . This study was carried out at the Faculty of Science, UTAR.

3.5.2 Scanning Electron Microscopy (SEM) and Energy Dispersive X-ray (EDX) Spectroscopy

The surface morphology analysis of the ZnO/ HAp samples was determined by using FESEM (Quanta FEG 450). The analysis was performed by evenly placing the developed powder of photocatalyst on a double sided carbon tape which was then attached to an aluminium sample stub. On the other hand, The EDX are utilized to determine the chemical compositions of ZnO/HAp photocatalyst via Oxford Instrument 50mm² supplied from United Kingdom. This study was carried out at Faculty of Engineering and Science, UTAR.

3.5.3 Fourier Transform Infrared Spectroscopy (FTIR)

FTIR analyses of ZnO/HAp photocatalyst was carried out to investigate the functional group. The FTIR data were scanned from 4000 cm^{-1} to 400 cm^{-1} . The analysis were carried out at Faculty of Science, UTAR.

3.5.4 Ultraviolet-visible Diffuse Reflectance Spectroscopy (UV-vis DRS)

The UV-vis DRS analysis was conducted using Perkin Elmer Lambda 35 to measure the characteristic of reflectance spectrum of the photocatalyst sampling was sent to Universiti Sains Malaysia.

3.5.5 Particle Size Analysis (PSA)

Particle Size Distribution (PSD) is conducted to determine different size of particle which are presented as proportions. The refractive index of the sample is first measured by the refractive index meter. Measurement is conducted by referring relative particle amount as a percentage where the total amount of particles is 100% in the sample particle group.

3.6 Photocatalytic Activity

The pollutant in the rubber wastewater as the pollutant in this reserach. Photocatalytic degradation by using ZnO/HAp photocatalyst were investigated in this study. The photocatalytic degradation of the photocatalyst was conducted in batch reaction system under UV irradiation with the apparatus set up shown in Figure 3.2. The experiment started with the preparation of 400 ml of glove wastewater in appropriate volume and distilled water. 400 ml substrate solution was prepared with 1g/L of photocatalyst as initial parameter was poured into a reactor. Air was supplied into solution mixture at an adjusted flow rate of 2.5 L/min throughout the experiment. The hot plate was using to ensure the continuous agitation at 350 rpm stirring rate throughout the experiment. 5 ml of suspensions from reaction mixture was taken at a fixed interval and utilizing syringe filters. The degradation efficiency was calculated using the equation below.

$$\text{Degradation efficiency} = \frac{C_o - C_t}{C_o} \times 100\% \quad 3.1$$

Where C_o indicates pollutant concentration after 30 minutes of dark adsorption and C_t indicates the pollutant COD level at reaction time, t (min)

3.7 Effect of HAp weight percent on ZnO/HAp nanoparticles

The effect of ZnO weight percent on ZnO/HAp photocatalyst on the photocatalytic degradation of rubber wastewater organic pollutants under UV irradiation was conducted in the range of 10 wt% to 50 wt%. The ZnO/HAp photocatalyst of different ZnO weight percent were synthesized by controlling the amount of HAp added correspond to 1g of ZnO

3.7.1 Effect of Catalyst Loading

The effect of catalyst loading on the photocatalysis of glove wastewater organic pollutants over the ZnO photocatalyst in the presence UV irradiation was experimented in the loading range of 1 g/L. The range was chosen refer to the literatures (Khezrianjoo & Revanasiddappa., 2013; Kansal, Kaur, & Singh., 2009). The experiment was conducted with initial wastewater concentration of 0.5 mg/L.

3.7.2 Scavenger Test

The radical scavenger experiment was conducted to indicate the importance and function of active species in the photocatalysis of glove wastewater over ZnO/HAp photocatalyst under UV irradiation. The reaction was carried out similarly except that 2mM of radical scavengers such as ethanol, potassium iodide and benzoquinone were added to rubber wastewater pollutants prior to addition of ZnO/HAp photocatalyst. The scavengers used for the photocatalytic degradation of glove wastewater were Isopropanol (IPA), Benzoquinone (BQ) and Ethylenediaminetetraacetic acid disodium salt (EDTA-2Na). The IPA was utilized to scavenge $\cdot\text{OH}$ radical, BQ was utilized to identify $\text{O}_2^{\cdot-}$ radicals and the EDTA-2Na was applied to detect h^+ in photocatalytic reaction. Other experiment parameters remain the same except for the presence of radical scavengers.

3.8 Phytotoxicity Testing

The phytotoxicity of the samples before and after glove wastewater degradation was examined using mung bean seeds. The surface of the seeds was first sterilized with NaOCl (0.5 wt%, 30 min). 9 green bean seeds were placed in each petri dish together with the cotton wool. In the defined time interval (12hr), the cotton was wetted using distilled water and incubated at room temperature for 6 days. After 6 days, the radicle length of each sample was measured and phytotoxicity was calculated by using equation

$$\text{Phytotoxicity (\%)} = \frac{\text{Radicle length of control} - \text{Radicle length of Sample}}{\text{Radicle length of Control}} \quad 3.2$$

CHAPTER 4

RESULTS AND DISCUSSION

4.1 Characterization

The characterization analyse of the Corn Husk ZnO phtocatalyst and Coupling of ZnO with HAp so as to describe their features. These analyses were X-ray diffraction (XRD), scanning electron microscope (SEM), energy dispersion X-ray (EDX) and transmission electron microscopy (TEM).

4.1.1 X-ray Diffraction (XRD)

The purpose of doing XRD analysis was to observed the crystalline structure of the zinc oxide photocatalyst. Figure 4.1 illustrates that XRD result of green synthesized corn husk ZnO, buffalo bone HAp and ZnO coupled with 50 wt% of HAp. The characteristic diffraction peaks at 31.84° , 34.5° , 36.34° , 47.62° , 56.68° , 62.92° , 66.46° , 68.04° , 69.2° can be matched to the diffraction plane of (100), (002), (101), (102), (110), (103), (200), (112), and (201), respectively. All this peaks were indicated that the hexagonal wurtzite Corn Husk ZnO crystal structure. The pattern spotted in the XRD result of the phase purity of the corn husk ZnO photocatalyst was proven that no additional crystalline impurities. Strong and narrow diffraction peaks that can observed from the result means the well crystalline of obtained photocatalysts. The XRD result of ZnO are similar to the results of several literatures. (Ghule et al., 2011; Miao et al., 2014).

The HAp crystalline structure was confirmed by the diffraction peaks observed at typical 2θ values of 26.08° , 31.96° , 40° , 46.88° , 49.66° which is similar result from the literatures. (Zhao et al., 2014). The diffraction peaks of ZnO/HAp XRD patterns revealed principal components of HAp and ZnO at figure 4.1. The crystallinity of the HAp in the ZnO-50%HAp structure can be indicated by the reflections observed at typical 2θ values 25.94° , 31.96° , 46.06° . Meanwhile, the narrow peak at 34.58° , 36.4° , 47.68° , 56.74° , 63.02° , 66.48° can be corresponded to the diffraction plane of (002), (101), (102), (110), (103), (200) respectively were attributed to the hexagonal structure of ZnO Np doped on the HAp. (Buazar et al., 2014; Ghule et al., 2011; Miao et al., 2014; Zhao et al., 2014)

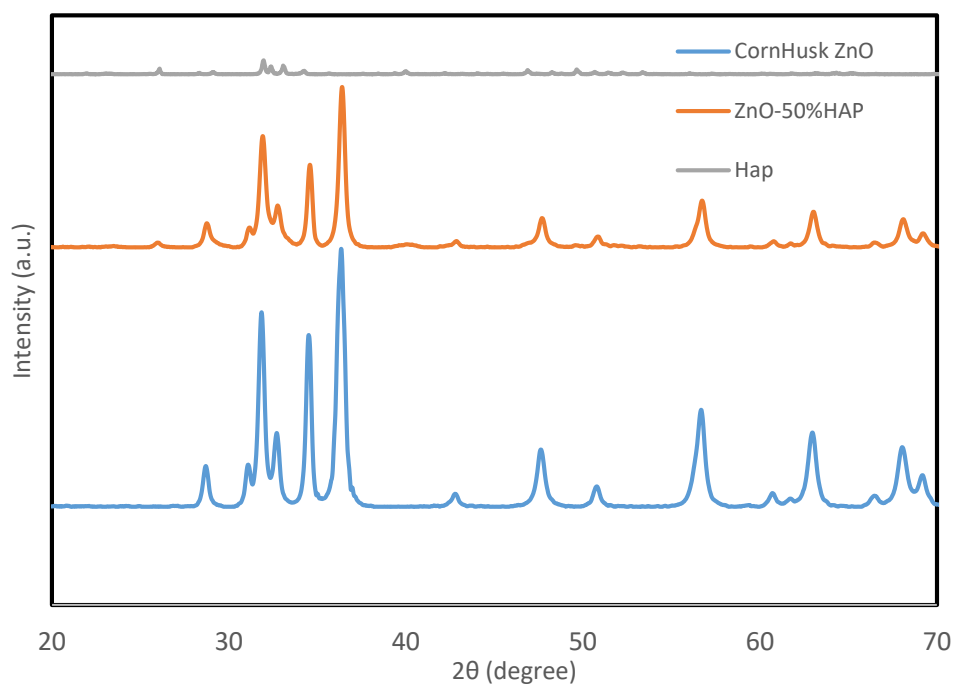
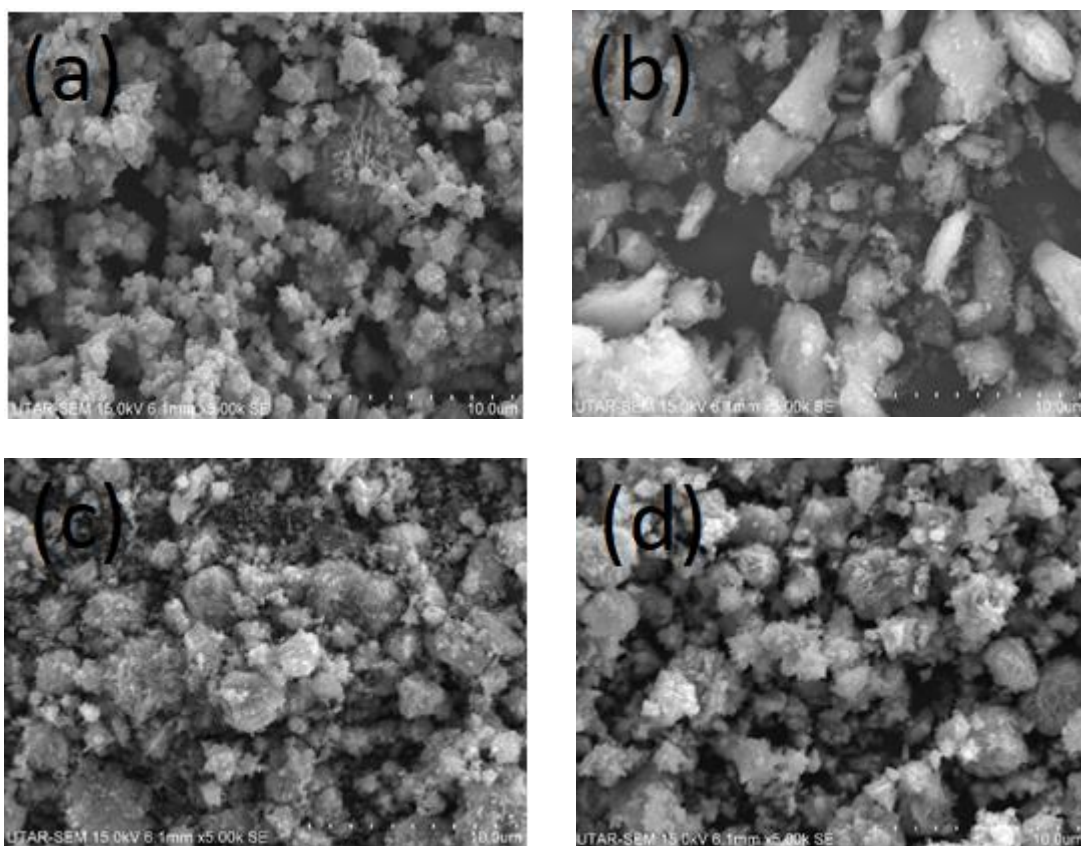


Figure 4.1: XRD pattern of ZnO, HAp, and ZnO-50%HAp

4.1.2 Scanning Electron Microscopy (SEM)

The morphology and nanostructure Corn Husk ZnO, HAp, ZnO/HAp nanocomposites were observed by SEM analyses. The SEM image of Hydroxyapatite(HAp), Corn Husk ZnO, Coupling of ZnO and weight percent of HAp was performed at the figure 4.2. From the figure 4.2, it was shown that the ZnO displayed as a flower shape structure whereas pure HAp appeared as oval shape nanostructure. Figure C to E shown the SEM image of the green synthesized coupled of ZnO/HAp photocatalyst with different weight percent of HAP. The ZnO were observed that well attached on the HAp nanostructure, indicating successful generated of ZnO/HAp nanocomposites. On the other hand, the HAp contact with the ZnO can help in promoting efficiency of transferring photo generated charge carriers and absorption efficiency.



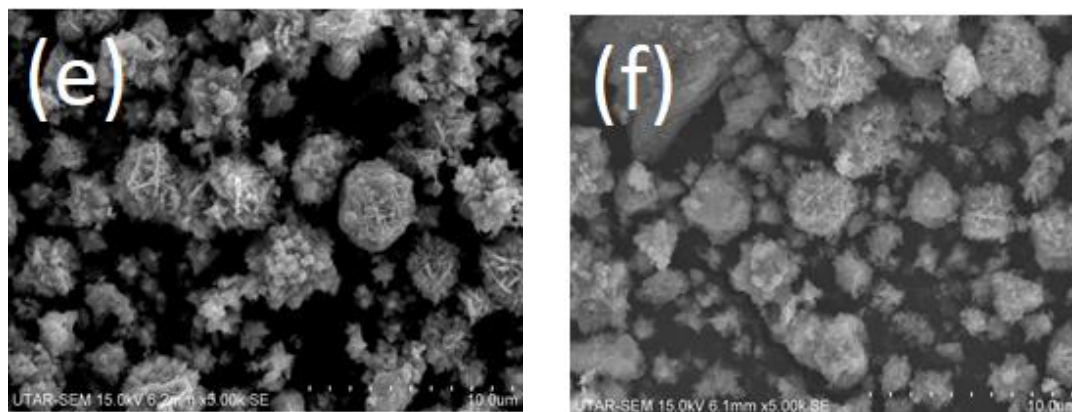
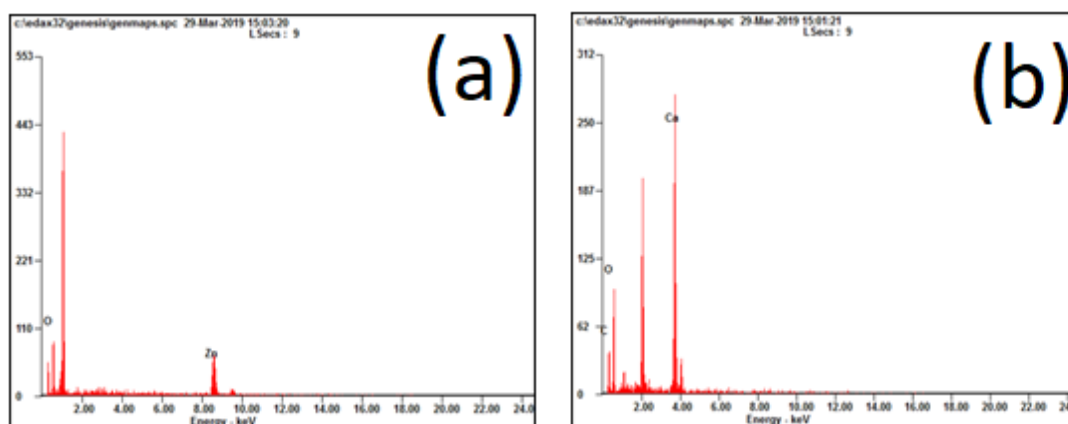


Figure 4.2: SEM image of Green Synthesized (a) Corn Husk ZnO (b) HAp (c) ZnO-20%HAp (d) ZnO-30%HAp (e) ZnO-40%HAp (f) ZnO-50%HAp photocatalyst at x5K magnification

4.1.3 Energy Dispersion X-ray (EDX)

EDX analysis was performed on the corn husk extract mediated ZnO, pure HAp and ZnO/HAp nanocomposites to confirm its elemental composition. According to the EDX analysis from figure 4.3, the peaks of Zn, O, Ca, P, H element can be easily observed. By referring to the result, the higher weight percent of ZnO coupled with the HAP was observed with more different peaks through EDX analysis owing to the presence of the elemental composition hydroxyapatite and ZnO. Furthermore, the C peak was also observed which can be originated from the supporting carbon tape.



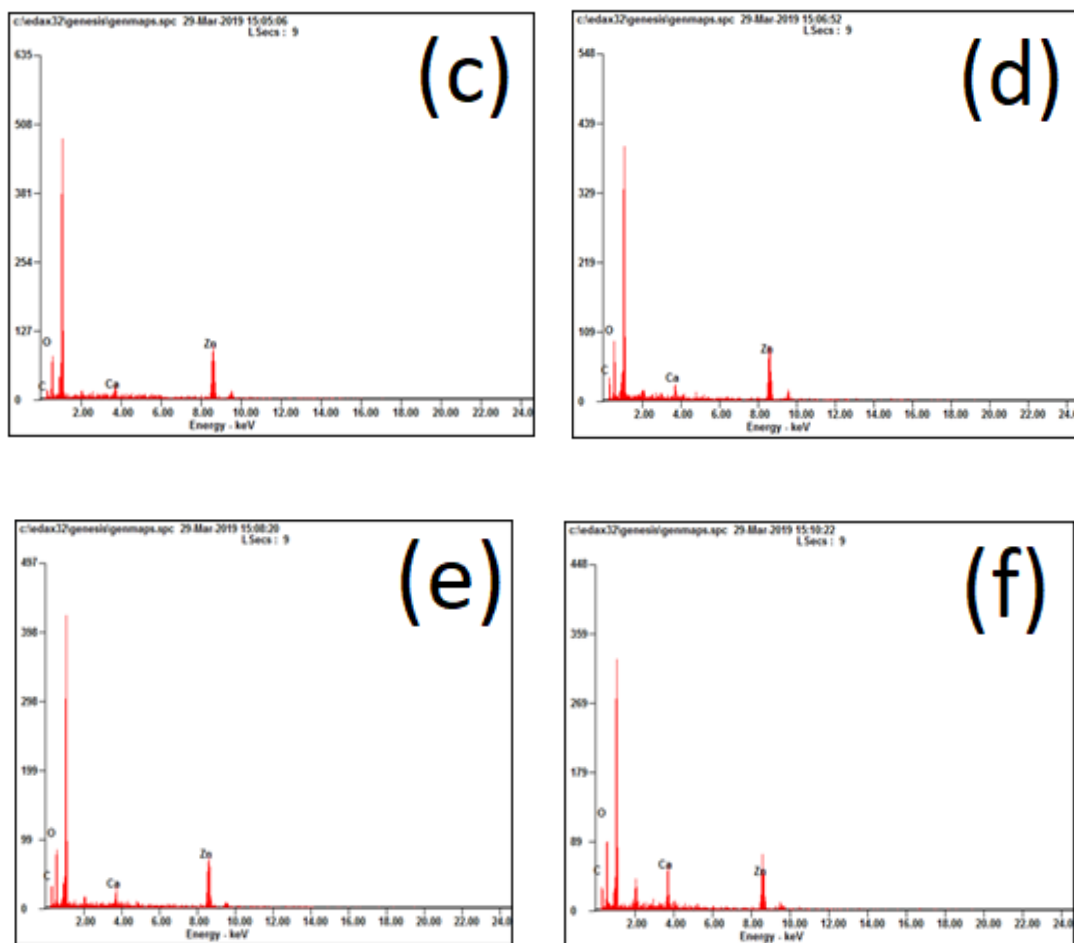


Figure 4.3: EDX spectrum of Green Synthesized (a) Corn Husk ZnO (b) HAp (c) ZnO-20%HAp (d) ZnO-30%HAp (e) ZnO-40%HAp (d) ZnO-50%HAp

4.1.4 Fourier Transform Infrared Spectroscopy (FTIR)

The FTIR spectra analyses show in the Figure 4.4 were the Corn Husk ZnO, HAp, ZnO-50%HAp. Purpose of doing FTIR analysis is to determine the nature and purity of the green synthesized corn husk ZnO, natural obtained HAp and Coupled ZnO with the HAp. Generally, metal oxide such as corn husk ZnO have absorption below 1000 cm^{-1} owing to the inter-atomic vibrations. The peaks detected from the Corn Husk ZnO (blue line) at 3854 cm^{-1} and 3402 cm^{-1} are owing to the O-H groups and H₂O molecules strongly bond to the catalyst surface (Xiong et al., 2006; Wahab et al., 2007). Additionally, a strong vibration band was observed at 497 cm^{-1} and 431 cm^{-1} which means distinct stretching mode of crystal ZnO and the characteristic absorption of ZnO bond. (Kadhim et al., 2015). Other peaks that observed in the corn husk ZnO at 1630 cm^{-1} were related to and hydroxyl surface functional group and 2369 cm^{-1} and 2345 cm^{-1} was indicated as presence of carbon dioxide impurities.

The result of the HAp in the FTIR spectra was observed. The first peak at the 3569 and 3648 cm^{-1} are due to the O-H stretching. Strong vibration band was detected in the HAp FTIR spectra at 1090 and 1046 cm^{-1} was indicated as the C-O stretching in the Hydroxyapatite. The peaks of 632 , 602 and 570 cm^{-1} that found in the FTIR spectra analysis of presence of impurities like alkenes. Referring to the FTIR result of ZnO-50%Hap, the first peak 3448 cm^{-1} presence was owing to the O-H group and H₂O molecules strongly bond to the catalyst surface and the peaks at 605 and 564 cm^{-1} is because of the presence of impurities (Xiong et al., 2006; Wahab et al., 2007). ZnO-50%HAp was coupling the ZnO and 50 wt% of HAp, so that the peaks observed at the 1090 and 1046 cm^{-1} indicate the C-O stretching of the hydroxyapatite and peaks at 485 and 431 cm^{-1} was because of the distinct stretching mode of crystal ZnO and the characteristic absorption of ZnO bond (Kadhim et al., 2015).

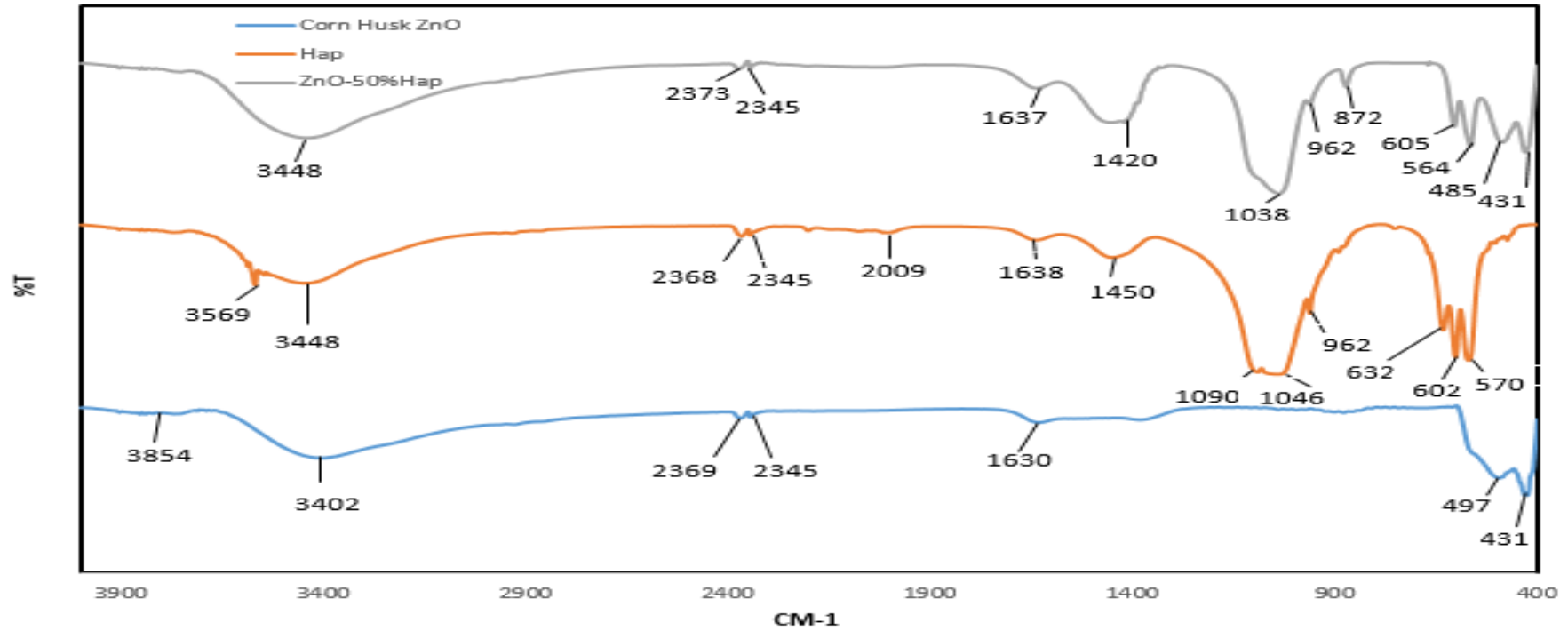


Figure 4.4: FTIR result of ZnO, HAp, ZnO-50%HAp.

4.1.5 Ultraviolet-visible Diffuse Reflectance Spectroscopy (UV-vis DRS)

The optical absorption spectrum of buffalo bone HAp, Corn Husk ZnO and ZnO-50wt%HAp photocatalyst was showed in Figure 4.5, 4.6 and 4.7. A trailing stream to the reflectance spectrum was detected near UV region which was a common trait of a semiconductor with a direct band gap (Lam et al., 2014). The light reflectance of the HAp, ZnO and ZnO-50%HAp increased steeply as it approaches 270 nm, 350 nm, and 290 nm respectively owing to the band gap transition. Consequently, the band gap energy can be calculated through the Equation 4.1 (Lam et al., 2014):

$$E_g = \frac{hc}{\lambda} \quad 4.2$$

Where

E_g = Band Gap Energy, eV

h = Planck's Constant (4.135667×10^{-5} eVs)

c = Light Velocity (3×10^8 m/s)

λ = Wavelength pf absorption, nm

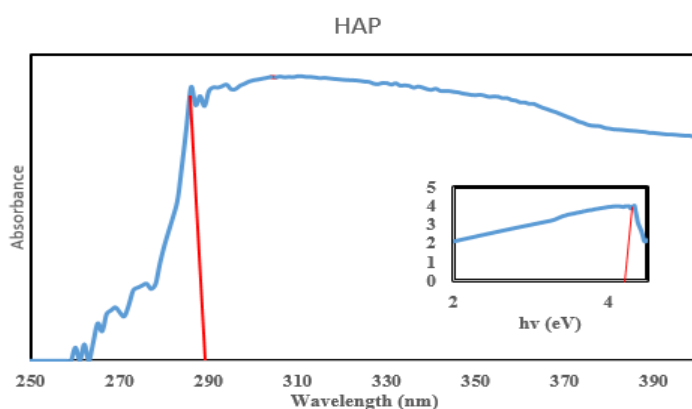


Figure 4.5: UV-vis DRS Spectrum of Buffalo Bone HAp

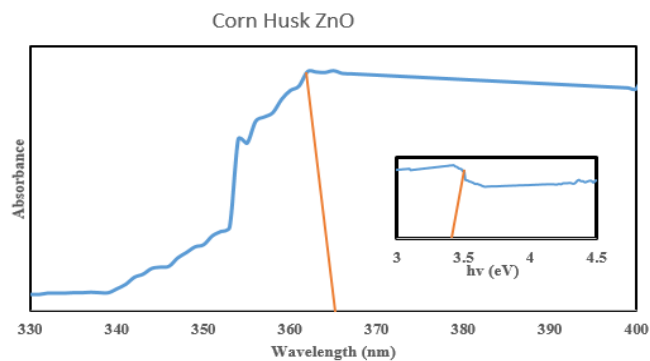


Figure 4.6: UV-vis DRS Spectrum of Green Synthesized Corn Husk ZnO

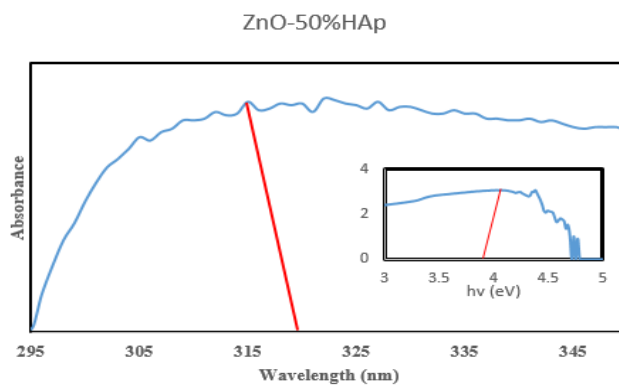


Figure 4.7: UV-vis DRS Spectrum of ZnO-50%HAp

It can observe that the absorption edge of HAp, Corn Husk ZnO and ZnO-50%HAp was approximately 290 nm, 365nm, and 320 nm respectively. By applying the equation 4.2, the measured band gap energy of HAp, Corn Husk ZnO and ZnO-50%HAp were 4.28 eV, 3.39 eV, 3.87 eV respectively. The band gap measurement result indicates that the ZnO after coupled with the HAp has higher band gap to absorb the light spectrum compare with Corn Husk ZnO. The pure HAp has the highest band gap energy which already exceed the UV light spectrum range for photocatalysis. These finding were similar with the literature report. (Buazar et al., 2014; Hu et al., 2018)

4.1.6 Particle Size Analysis

The particle size of the ZnO, ZnO-50%HAp and HAp were obtained in the result below. Referring to the figure 4.8, the particle size distribution of the ZnO, ZnO-50%HAp and HAp in the narrow particle size ranging from 0.04 to 0.316 μm . Summary of the physical properties of the photocatalyst obtained by the PSA were shown in the Table 4.1. The ZnO, ZnO-50%HAp and HAp particle distribution is narrow, with mean diameter 0.118, 0.118 and 0.150 respectively. Fine particle has higher specific surface area as compared to coarse particle. According to the physical properties obtained from the PSA analysis, the HAp ($39.9 \text{ m}^2/\text{g}$) has lower specific surface area than the ZnO ($50.7 \text{ m}^2/\text{g}$) and ZnO-50%HAp ($50.8 \text{ m}^2/\text{g}$) which means the HAp are coarser particles.

Table 4.1: Refractive Index

Sample	Refractive Index
Corn Husk ZnO	1.337
HAp	1.334
ZnO-50%HAp	1.337

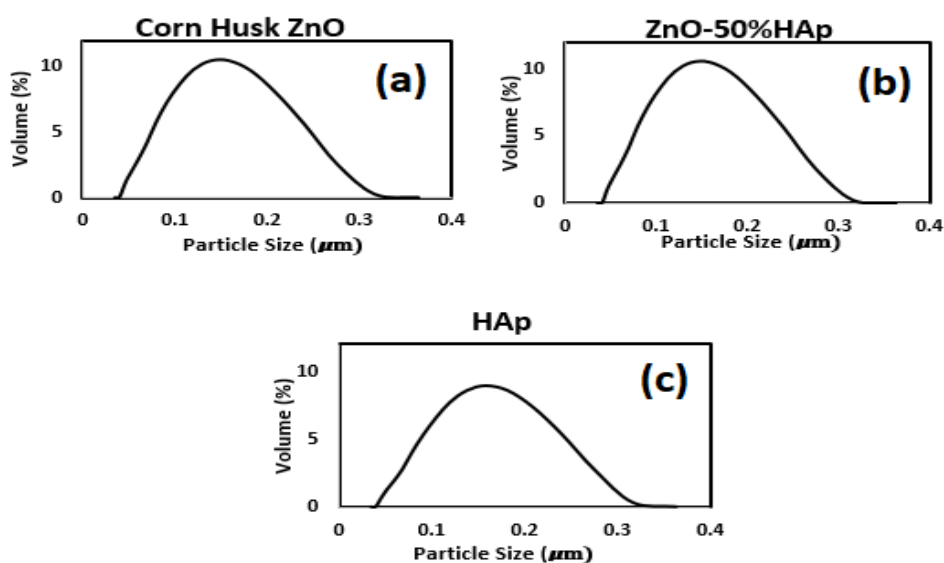


Figure 4.8: Particle Size Analysis of (a) Corn Husk ZnO (b) ZnO-50%HAp and (c) HAp

Table 4.2: Physical Properties of the Photocatalyst

Sample	Physical Properties	
	Mean Diameter (μm)	Specific Surface Area (m^2/g)
Corn Husk ZnO	0.118	50.7
HAp	0.118	50.8
ZnO-50%HAp	0.150	39.9

4.2 Control Experiment

At the starting stage of photocatalytic degradation, three set of control experiments were conducted to determine the effect of dark adsorption, photolysis and photocatalysis. In the preliminary step, 10 ppm of diluted glove wastewater and ZnO photocatalyst loading of 1 g/L were used for the photocatalytic degradation experiment. Photolysis degradation of glove wastewater was studied by conducting the experiment in the presence of UV Lamp irradiation without using photocatalyst. The semiconductor catalyst was used to study the effect of dark adsorption without UV lamp irradiation. The purpose of the dark adsorption is to study the catalyst adsorption when the dark run with only presence of the photocatalyst. On the other hand, the photocatalytic degradation was carried out by using ZnO photocatalyst and presence with the UV lamp irradiation. Figure 4.6 show the degradation efficiency of the glove wastewater under different control process condition.

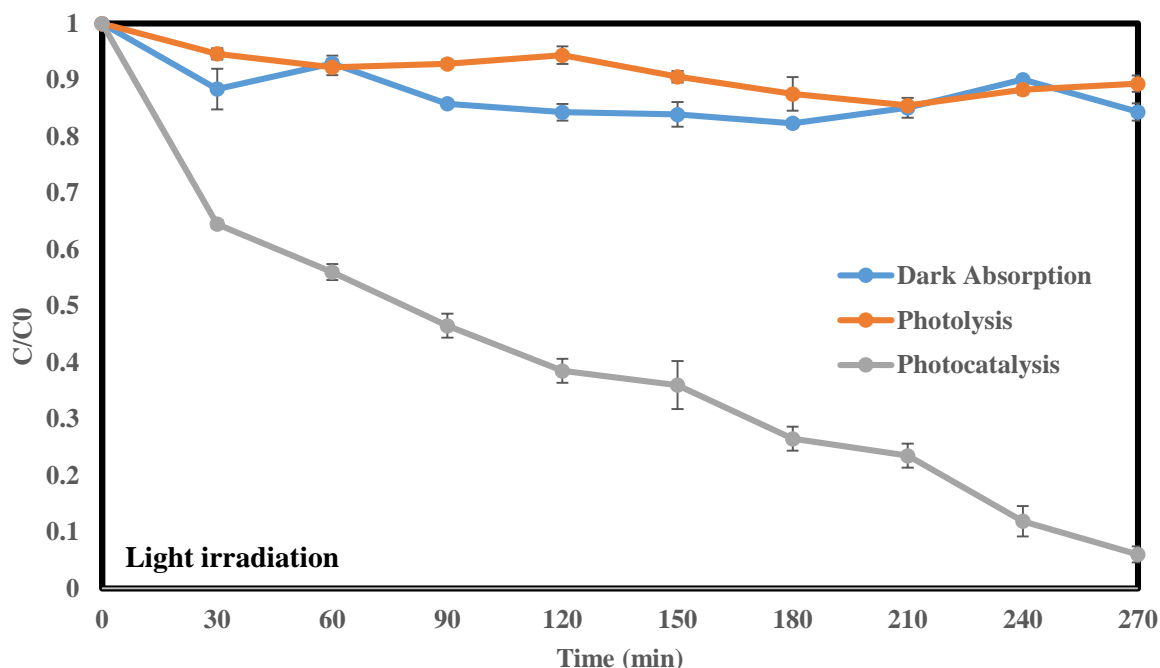


Figure 4.9: Photocatalytic Degradation of Glove Wastewater under different conditions. Condition: Diluted initial 10 ppm Glove Wastewater, ZnO-50%Hap Catalyst Loading=1g/L.

By referring to Figure 4.6., the dark adsorption and the photolysis degradation were running very slow because the concentration of glove wastewater after the experiment remained almost unchanged. In the dark adsorption, it only has low degradation performance of 8.07%. Concentration of the glove wastewater was just slightly decreased inside the dark adsorption owing to the adsorption of organic compounds on the photocatalyst surface. The result also similar with the research from Mohsin, Juda, & Mashkour (2013). In their research, they have conducted the dark run of degradation by using Sunset Yellow Dye over similar ZnO photocatalysis. The result in their study reported the reduction efficiency of 8.53% at the first 30 min. This result proved that the reduction in Sunset Yellow pollutant concentration because of the adsorption of dye pollutants on the ZnO photocatalyst and there was no photocatalytic degradation occur (Mohsin, Juda., & Mashkour., 2013). The photolysis degradation of the glove wastewater in this study was negligible. The degradation efficiency of the photolysis in this study is only 0.7 % under the UV irradiation. Small reduction in glove wastewater concentration proved that the photolysis degradation showed negligible interference of photocatalytic degradation.

The photocatalytic degradation by Corn Husk ZnO photocatalyst under the UV irradiation reached the highest degradation of the glove wastewater. The photocatalytic degradation achieved almost complete degradation of textile dye inside the glove wastewater at 300 min. It is obvious the use of green synthesized ZnO semiconductor catalyst have large improved the photocatalytic degradation. This is owing to the photoexcitation of a semiconductor during the solar energy irradiation. The energy state of electrons was promoted along with the generation of electron-hole pair on the catalyst surface with the illumination of photocatalyst with light irradiation. The presences of the electron-hole pair on the catalyst surface which can enabled the generation of strong oxidizing agents (.OH radical) that are functioned to degrade the organic pollutants. Therefore, high degradation efficiency of the glove wastewater can be achieved when there is presences with both light and semiconductor catalyst. Compare the results of photolysis, dark absorption and photocatalytic degradation observed that the organic pollutants degradation experiments were conducted at an almost pure photocatalytic condition (Ahmed et al., 2010; Lam et al., 2012; Ribeiro et al., 2015)

4.3 Effect of Hap Content in ZnO

In this research, it is important to study the effect of HAp content in the ZnO/HAp nanocomposites on the photocatalytic degradation of glove wastewater. The coupling of the Hydroxyapatite (HAp) and Zinc Oxide (ZnO) was varied with the weight percent of the HAp. The HAp content in ZnO/HAp photocatalyst was varied from the 20 wt% to 50 wt%. Figure 4.7 shows the photocatalytic degradation efficiency of glove wastewater using ZnO/HAp with different weight percent of HAp. In this experiments, the samples include Corn Husk Pure ZnO, ZnO-20%HAp, ZnO-30%HAp, ZnO-40%HAp, ZnO-50%HAp and Pure HAp.

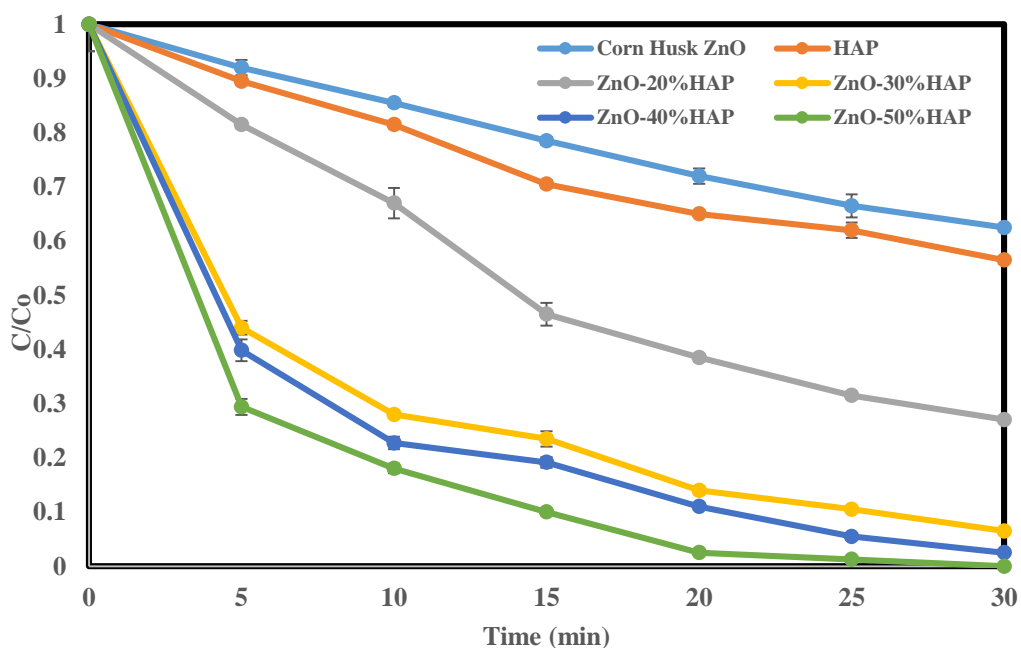


Figure 4.10: Effect of Hap content in ZnO/Hap nanocomposites for photocatalytic degradation of glove wastewater. Conditions: Diluted 10 mg/L glove wastewater, 1g/L catalyst loading.

In the first 30 min, the degradation efficiency for all sample is low for the dark absorption. The experiments conducted with Corn Husk ZnO and Pure HAP semiconductor catalysts showed low glove wastewater degradation efficiencies of 62.5% and 56.5% respectively under a 30 min UVc Lamp photocatalytic degradation.

As for the photo degradation using the ZnO couple with the Hap (ZnO/HAp) with different weight percent of HAp showing the higher photocatalytic degradation efficiency. The ZnO-20%HAp showed the moderate degradation efficiency of 27% under photocatalysis. The ZnO/HAp with higher percentage of Hap than 20% (30%, 40%, and 50%) showed higher photocatalytic degradation efficiency. The ZnO-30% and ZnO-40% have reached the very high degradation efficiency of 93.5% and 97.5% in 30 min. Based on the figure shown that, the highest photocatalytic degradation efficiency of the glove wastewater is the ZnO-50%HAP. ZnO-50%HAP fully degrade the glove wastewater under the presence of UV lamp in 30 min. The higher content of hydroxyapatite couple with the ZnO, it will enhance the adsorption surface to improve the degradation efficiency as well. Therefore, the highest content of the Hap couple with the ZnO showed the highest photodegradation efficiency.

The effect of HAp content in the ZnO/HAp photocatalyst on the photocatalytic degradation of glove wastewater was explained in terms of adsorption ability and the effectiveness of charges carrier. The presences of the Hap will enhanced the photocatalytic degradation owing to the surface adsorption ability. Besides, the UV irradiation of the photocatalytic degradation leads to create an O vacancy in the hydroxyapatite lattice. The hydroxyapatite vacancy leads the transfer of an electron to the atmospheric oxygen which generate the charged O_2^- species. The O_2^- species will react with the liquid/ gaseous molecules and degrade them. According to the figure, the degradation efficiency of glove wastewater increased as the HAp content increased from 20wt% to 50wt%. The degradation efficiency is low when the HAp content is low. This is owing to the low content of HAp will led the unobvious charge carrier's separation effect and the lower light absorption ability. When the HAp content is increased to 50 wt%, it will substantially increase the light absorption in the UV, which will also increase the electron transfer to the atmospheric oxygen which generate more charged O_2^- to enhance the photocatalytic degradation efficiency. The higher HAp content also will improve the efficiency of interfacial charge transfer which will have resulted in better photocatalytic properties. This is owing to the recombination of photo-generated electron and hole will inhibited (Lam et al., 2012). Besides that, the addition of HAp also can improve the adsorption of organic pollutants to the surface of ZnO. As HAp is an adsorbent, more

pollutants on the surface of ZnO can accelerate the contact of pollutant and radicals on the photocatalyst surface which lead to higher activity. The pollutant absorbed by HAp will be suggested to migrate to photocatalyst surface. The studied carried out by the (Buazar et al., 2014) proved that the ZnO dope with the HAp will enhance the photocatalytic reaction than single ZnO and HAp. In their results, the ZnO/HAp has the highest removal efficiency of 2-mercaptobenzoxazole (MBO) (99.45%) under UV irradiation. The trend of photocatalytic activity of their studied nanophotocatalyst for degradation MBO was ZnO/HAp > ZnO > HAp.

4.4 Radical Scavenger Test

It was generally accepted that the photocatalytic degradation involved massive amount of main reactive oxygen species including O_2^- radicals, $\cdot OH$ radicals and h^+ . Thus, the effects of different of radical scavengers on both photodegradation of pre-treated glove wastewater were evaluated in attempt to explain the reaction mechanism. Therefore, scavenger test is carrying out to indicate the role of each active species in assisting in photocatalytic degradation of glove wastewater. This test also aimed to determine the degradation efficiency in the absence of these active species by eliminating them through addition of scavengers. The scavengers used for the photocatalytic degradation of glove wastewater were Isopropanol (IPA), Benzoquinone (BQ) and Ethylenediaminetetraacetic acid disodium salt (EDTA-2Na). The IPA was utilized to scavenge $\cdot OH$ radical, BQ was utilized to identify O_2^- radicals and the EDTA-2Na was applied to detect h^+ in photocatalytic reaction. All the experiments were conducted at with 10 mg/L initial concentration of glove wastewater and 1 g/L of catalyst loading.

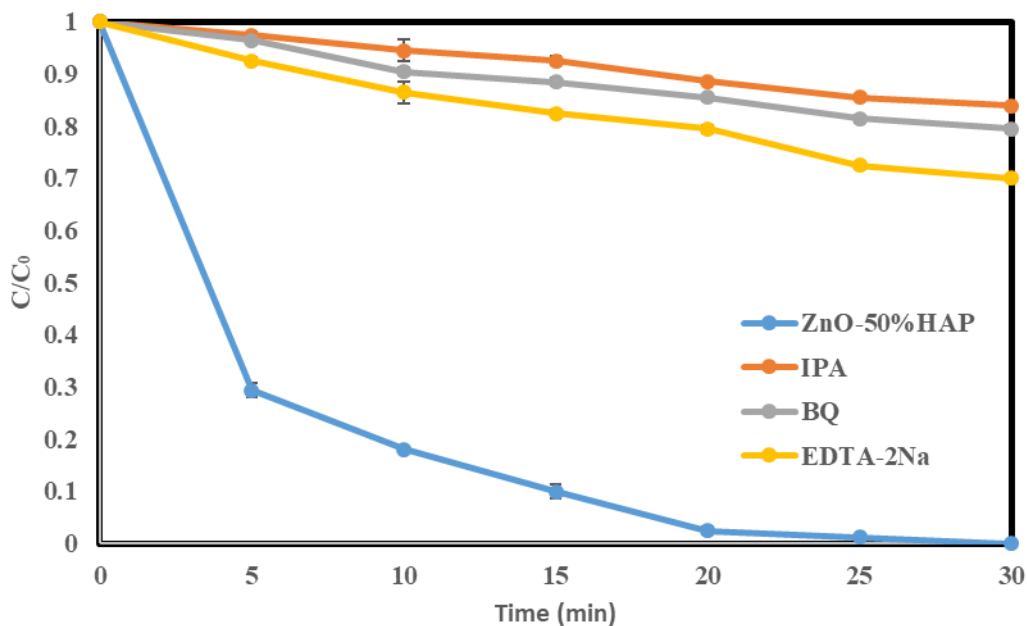


Figure 4.11: Effect of radical scavengers testing at 0.5Mm on UV irradiation degradation of glove wastewater over ZnO nanocomposites. Conditions: Diluted 10 mg/L Initial glove wastewater concentration and 1g/L of catalyst loading.

Influence of a series of scavengers on the COD removal efficiency of glove wastewater using the ZnO/HAp semiconductor catalyst is shown in the figure 4.8. From the result, the experiments without presence any scavengers showed the best degradation performance among the other three set experiment without presence of scavengers. The experiment without presence of any scavengers perform with 100 % of COD removal efficiency compared to 16%, 20.5% and 30% for IPA, BQ and EDTA-2Na respectively. All three oxidative species also performed their roles in photocatalysis as the reduction was significant as compared to 100%. Addition of the IPA scavenger was largely inhibited the COD removal of glove wastewater. Implying that the $\cdot\text{OH}$ radicals were the dominant reactive species partook in the photocatalytic process and also play larger role in the photocatalytic degradation of glove wastewater. Although, addition of BQ and EDTA-2Na decrease the COD removal efficiency of glove wastewater to lesser extent, which demonstrated that the O_2^- radicals and h^+ played minor roles on the photocatalytic degradation of glove wastewater. Referring to the research from Yang et al (2017), the similar degradation result on the photodegradation of methylene blue (MB) was obtained. Their study

reported that addition of tert-butyl alcohol which was similar with the IPA as a $\cdot\text{OH}$ radicals scavenger into the reaction system, the degradation of MB decreased significantly from 44.5 % to 12.5% as compared with addition of benzoquinone which resulted in drop of degradation efficiency from 44.6% to 34.6% (Yang et al, 2017). The research from the Djebbar, Zertal and Sehili (2006) also showed that the degradation of glove wastewater was inhibited by 70% in the presence of ethanol which is similar with IPA as $\cdot\text{OH}$ radical scavengers. The ethanol reduced the degradation efficiency due to the absence of $\cdot\text{OH}$ radicals to oxidize the organic pollutant. Besides that, another study use the potassium iodide which is similar with EDTA-2Na to scavenge h^+ ion owing to its efficient formation of I_2 and $I_2^{\cdot-}$ was shown in the scavenger reaction sequences below. (Equations 4.1-4.3) (Palominos et al, 2009; Sin et al, 2014).



In the photocatalytic degradation , BQ was often used as scavenger to investigate the effect of $O_2^{\cdot-}$ radicals owing to its capability to trap all the radicals by electron transfer mechanism that showed in equation 4.4 (Palominos et al, 2009; Palaez et al, 2012; Sin et al, 2014).



Photocatalytic degradation of glove wastewater over ZnO nanocomposites under presence of different scavengers at 0.5 mM were shown in Figure. The experiments were conducted with 10 mg/L initial glove wastewater concentration, 1 g/L catalyst loading.

4.5 Phytotoxicity

Wastewater that discharge from the glove industry may contain some chemical that will lead the damage of aquatic life and serious environmental pollution. The chemical content inside the glove wastewater include of nitrogenous compound. To study the phytotoxicity of samples before and after photocatalytic degradation of the glove wastewater by using the mung bean seeds. The figure 4.9 showed the obtained result of phytotoxicity of samples. Referring to the result, it can be seen that there was an observably decrease in phytotoxicity of the samples after degradation. The calculated phytotoxicity level of 63.15 % was obtained for the samples after degradation, while the samples before degradation has phytotoxicity level of 100%.

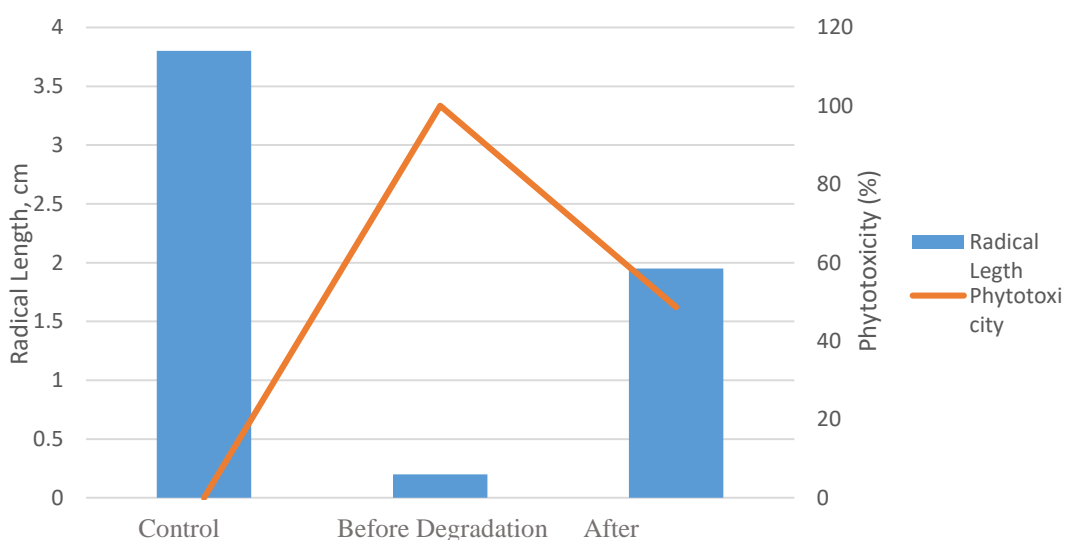


Figure 4.12: Phytotoxicity Test

After the 6 days period for conduct the experiment, the radical length was observed from the sample after degradation was 1.4 cm. The mung bean seeds treated with the samples before degradation showed the 0.2 cm radical length. The radical length for the samples after degradation reduced almost 50% from the radical length in the control. This result indicates that the effectiveness of photocatalytic degradation of glove wastewater using ZnO-50%HAp as photocatalyst. The figure

4.9 also showed the observed condition of mung bean seeds indifferent samples after 6 days growth. Referring to study of the Samir et al,2015, the phytotoxicity testing on the lepidium sativum seeds by using TiO_2 as photocatalyst. The results in this study showed that the stem inhibition up to 85% was recorded for the samples of glove wastewater before undergoing photocatalytic degradation.

4.6 Effect of Operating Parameter

In our research, there are 2 significant parameters for study the process parameter which are initial wastewater concentration and catalyst loading.

4.6.1 Effect of initial wastewater concentration

The dependency of the photocatalytic degradation of glove wastewater on the initial concentration was investigate in the presence of 1g/L of catalyst loading. The catalyst using in this experiment was the optimum degradation efficiency coupling ZnO-50wt%HAp. The effect of the initial wastewater concentration on the photocatalytic degradation was observed by varying the initial wastewater concentration from 10 mg/L to 50 mg/L. Figure 4.10 illustrates the performance of the photocatalytic degradation with different initial wastewater concentration with constant 1g/L catalyst dosage.

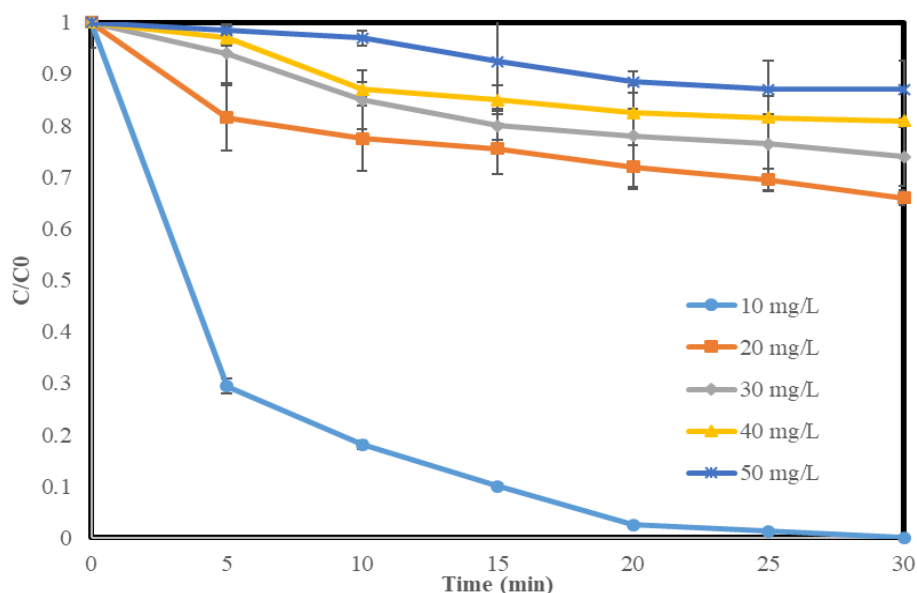


Figure 4.13: Effect of initial glove wastewater Concentration on the photocatalysis of glove wastewater over ZnO/HAp nanocomposites. Conditions: 1g/L catalyst loading.

From the result, it can be noted that the degradation efficiency at low glove wastewater concentration of 10 mg/L (100% COD removal efficiency) was higher than the 20 mg/L (44 % COD removal efficiency), 30mg/L (26% COD removal efficiency), 40 mg/L (19.05% COD removal efficiency) and 50 mg/L (13 % COD removal efficiency) of glove wastewater concentration. Therefore, the lowest initial wastewater concentration (10 mg/L) demonstrated best photocatalytic activities as compared with other higher initial wastewater concentration. This was owing to the light cannot pass through the high concentration at dark environment. The degradation efficiency would be higher when the pollutant to be degraded is lesser. This also can be explained in the studies by Subash et al (2013). In their studies, the better photocatalytic degradation efficiency was evaluated when there is presence of less pollutants. Their results display the highest photocatalytic degradation efficiency was observed when there was low concentration of 1×10^{-4} M Acid Black 1 dye with 3 g/L WO₃-Ag-ZnO under 30 min compared to other higher dye concentration.

In addition, low initial wastewater concentration allowed less interface of less pollutants inside the glove wastewater towards the light photons. It would allow more photons to attach to the surface of the semiconductor catalyst for production of photogenerated e_{CB}^- thus amplifying the photocatalytic efficiency (Chamjangali and Boromund., 2013). The other studies carried out by the Yang et al (2017) also reported that the degradation efficiency of Rhodamine B dye under photocatalytic degradation over ZnO nanorods decreased from the 93.31% to 27.82% when the wastewater concentration varied from 10 mg/L to 50 mg/L.

The phenomenon where the degradation efficiency decreased when the initial wastewater concentration increased could be due to decrease in the concentration of generated active radicals. The intermediate product that released from the wastewater pollutants would compete with the pollutants for available ZnO/HAp active sites. The higher amount of the pollutants molecules would be attached to the active sites of the photocatalyst as dye concentration. This will increase the competence between the pollutants and photocatalyst and reduce the degradation efficiency. The higher the concentration of the wastewater concentration will generate more intermediate

product which would reduce the degradation efficiency since the available amount of active sites is fixed with continuous UV light intensity.

The 10 mg/L of initial wastewater concentration showed the 100% degradation efficiency under 30 min owing to the lesser pollutants in the system compared to other varied initial wastewater concentration. The competition with O_2 and OH^- ions on the surface of photocatalyst would be less when the presence of pollutant in lesser amount. Referring to the research paper that conducted by the Khatee et al (2014), low dye concentration of Acid Red 17 dye as less amount of dye molecules were attached at the active sites of catalyst would lead to high photocatalytic degradation efficiency of 67% Acid Red 17 dye. This is owing to the vacant active site of catalyst would generate $\bullet OH$ radicals from O_2 and OH^- ions which will lead to higher photocatalytic degradation. As a result, the 10 mg/L of initial wastewater concentration was selected as it showed the optimum COD removal efficiency of glove wastewater compare to other initial glove wastewater concentration.

4.6.2 Effect of Photocatalyst Loading

Photocatalyst loading in photocatalytic process is one of the important factor that can influence the efficiency of glove wastewater degradation. Therefore, it is important to obtain the optimum amount of catalyst loading in photocatalytic process. In this experiments, the catalyst loading for the photocatalytic process was varied from the 0.5 g/L - 1.5 g/L of ZnO-50% HAP and the COD reduction after 30 min irradiation. Figure 4.11 shows the COD removal efficiency of glove wastewater under different amount of ZnO nanocomposites photocatalyst. Based on the results shown in figure 4.14, the COD removal efficiency of the glove wastewater increased from the 56.5% to 100% when the photocatalyst loading increased from 0.5 g/L to 1 g/L. However, the COD removal efficiency dropped from 100% to 81.6% when the catalyst loading

reached 1.5 g/L. Therefore, the optimum value of the ZnO-50% HAp nanocomposites photocatalyst to degrade the glove wastewater was 1 g/L.

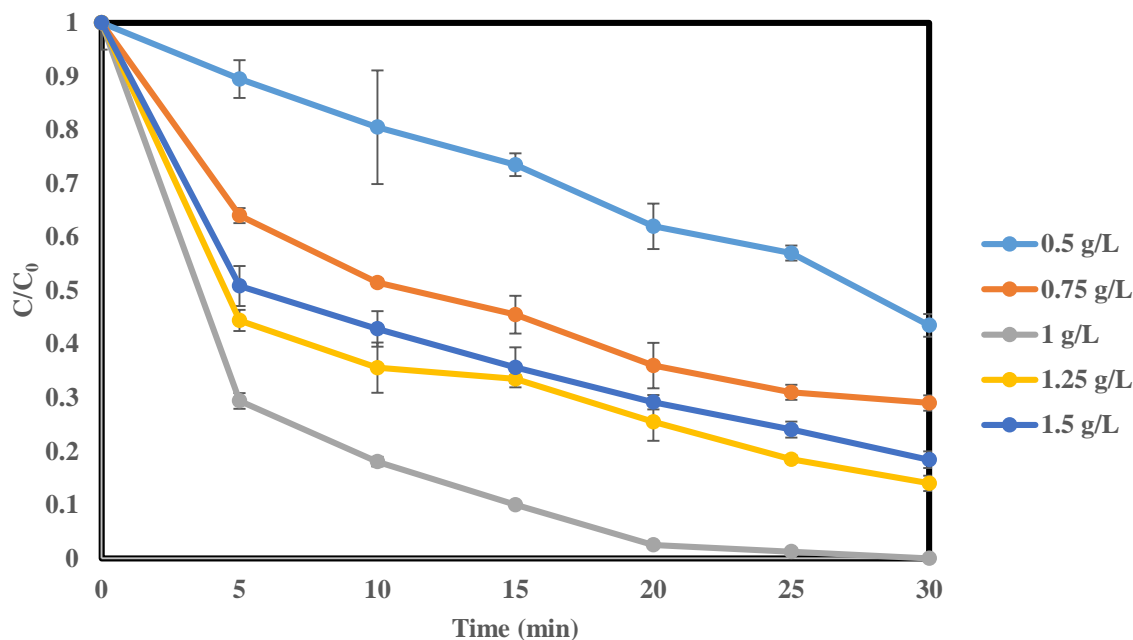


Figure 4.14: Effect of Photocatalyst Loading on Photocatalysis of Glove Wastewater over ZnO/HAp nanocomposites. Condition: 10 mg/L of initial wastewater concentration.

The effect of photocatalyst loading on the glove wastewater can be described in terms of the amount of active sites available, absorption area available for generate active radicals and the amount of light can be penetrated. As the amount of catalyst increased, the amount of the active site available on the photocatalyst surface increased and resulting higher adsorption area that is available for the formation of active radicals to degrade the pollutant (Ahmad et al., 2010; Lam et al., 2012). The studies from Chen et al (2011) was conducted the photocatalytic degradation of methyl orange by ZnO and varied with the amount of catalyst loading. Their study reported that the photocatalytic degradation efficiency increased when photocatalyst loading increase to an optimum value of 2.5 g/L. This is owing to the amount of active surface area of the photocatalyst ZnO nanocomposites available increased.

Nevertheless, the catalyst loading increase over certain amount was led to reduction of the degradation efficiency. This is owing to the light scattering effect and increase in the aggregation of photocatalyst. Another study by Kansal, Kaur & Singh (2009) was obtained the similar result on the photocatalytic degradation of Reactive Orange 4 Dye over ZnO photocatalyst. Their study showed that the excess loading of photocatalyst leading an increase in the turbidity level of the mixture and decrease the light penetration decreased. Thus, resulted in lower degradation efficiency.

Commonly, the optimum loading of photocatalyst for ZnO based photocatalyst was observed to be 0.16 g/L to 10.0 g/L from various studies from previous study which was reliant on on the nature, of photocatalyst, reactor configuration, light energy and pollutants (Jiang et al., 2008; Lam et al., 2012; Rao et al., 2012). Consequently, the optimum loading for the ZnO/HAP photocatalyst in this study was 1.0 g/L.

4.7 Glove wastewater characteristic

Table 4.3: Comparison of raw glove wastewater and degraded glove wastewater after 30 min irradiation time. (COD of raw discharged glove wastewater = 1254 mg/L)

Parameter	Initial Wastewater (Diluted to 10 ppm)	Degraded Wastewater after 30 min	Removal efficiency
Turbidity (NTU)	32.1	10.65	66.8%
Colour (Pt-Co)	42	13.62	67.5%
Ammonia (NH ₃ -N)	1.03	0.53	48%
TSS (g)	0.0152	0.003	80.3%
pH	11.48	8.03	-
COD (mg/L)	10	0	100%

Removal efficiency of the turbidity, colour, Ammonia, and TSS after 30 minutes of UV irradiation time were observed as 66.8%, 67.5%, 48% and 80.3% respectively. The complex functional group of different dyes and presences of inorganic ions such as Cl⁻ will indirectly affect photodegradation of glove wastewater. The pH of the glove wastewater was recorded reduction from 11.48 to 8.03 could be attributed to the generation of aliphatic carboxylic acid that converted from the destroyed intermediate during photocatalytic degradation. (Delnavaz et al., 2012)

CHAPTER 5

CONCLUSION AND RECOMMENDATIONS

5.1 Conclusion

In our research, zinc oxide (ZnO) has been successfully synthesized through corn husk extract. This study focuses the green synthesized method through plant mediated extract to synthesized the photocatalyst and thus achieved the generation of environmental friendly and low cost semiconductor catalyst. Furthermore, the Hap obtained from the buffalo bone was utilized to doped with ZnO as photocatalyst support to enhance the adsorption of pollutant and photocatalytic activity. ZnO was doped with Hap through sonication to form coupled ZnO/HAp. This project also studies the effect of HAp weight percent in ZnO content to observed the optimum weight percent of ZnO to enhance the photocatalytic degradation and has been characterized. Result from the scanning electron microscopy (SEM) image, microflower structure ZnO was found to be adhering on two the Hap with pellet shape three dimensional nanocomposites structure, which represent successful coupling of the catalyst and the catalyst support. In addition, the energy dispersion X-ray (EDX) spectrum of ZnO/HAp revealed the presences of different composition, which were Zn, O, Ca, P, H in the plant mediated extract synthesized photocatalyst. Based on the X-ray diffraction (XRD) pattern of ZnO, HAp, and ZnO-50%HAp photocatalyst, the clear and intense diffraction peaks indicated the well-crystalline hexagonal wurtzite structure of ZnO.

Fourier Transform Infrared Spectroscopy (FTIR) was also carried out to indicate the composition of photocatalyst Zn-O bond and Zn-O-HAp bond were found in the infrared spectrum.

The control experiment in this study revealed the low degradation efficiency of glove wastewater during the photolysis and dark adsorption compared to photocatalysis. Additionally, the effect of HAp weight percent in the green synthesized ZnO/HAp catalyst on the degradation of glove wastewater was also studied. In this study, the ZnO weight percent was varied from 20wt % to 50wt%, the completely COD removal efficiency was achieved when the HAp weight percent reached 50wt%. Therefore, the optimum Hap weight percent in ZnO/HAp catalyst was found to be 50 wt%.

Besides that, the role of each active species in photocatalysis of glove wastewater using ZnO/HAp as photocatalyst under UV light irradiation was also through scavenger's test. All three oxidative species, which are Isopropanol (IPA), Benzoquinone (BQ) and Ethylenediaminetetraacetic acid disodium salt (EDTA-2Na) also performed their roles in photocatalysis as the reduction was significant as compare to 100%. The result showed that each active species played its role in assisting photocatalytic degradation of glove wastewater. Nevertheless, EDTA-2Na as a h^+ radical scavenger, was found to have more obvious inhibition effect on the degradation of glove wastewater as its degradation efficiency dropped from 100% to 70% compared to isopropanol and benzoquinone which gave removal efficiency of 84% and 79.5% respectively.

5.2 Recommendation

Few recommendations were suggested for the use of the future research:

1. Current study on effect of HAp weight percent in coupled ZnO/HAp catalyst was shown to have significant impact on photocatalytic degradation of glove wastewater. However, the effect of adsorption and desorption study of ZnO/HAp catalyst, optimum time of photocatalysis, solution pH, light intensity, presence of oxidizing agent were not evaluated yet. Therefore, systematic study can be performed to understand the impact of these parameters on the degradation performances.

REFERENCES

- Abdul Salam, H., Sivaraj, R. and Venckatesh, R., (2014). Green synthesis and characterization of zinc oxide nanoparticles from *Ocimum basilicum* L. var. *purpurascens* Benth.-Lamiaceae leaf extract. *Materials Letters*, 131, pp.16-18.
- Anbuvaran, M., Ramesh, M., Viruthagiri, G., Shanmugam, N. and Kannadasan, N., (2015). Synthesis, characterization and photocatalytic activity of ZnO nanoparticles prepared by biological method. *Spectrochimica Acta Part A: Molecular and Biomolecular Spectroscopy*, 143, pp.304-308.
- Anbuvaran, M., Ramesh, M., Viruthagiri, G., Shanmugam, N. and Kannadasan, N., (2015). *Anisochilus carnosus* leaf extract mediated synthesis of zinc oxide nanoparticles for antibacterial and photocatalytic activities. *Materials Science in Semiconductor Processing*, 39, pp.621-628.
- Adollahi, Y., Abdullah, A.H., Zainal, Z. and Yusof, N.A., (2011). Photocatalytic Degradation of P-cresol by Zinc Oxide under UV irradiation. *International Journal of Molecular Sciences*, 13(1), pp.302-315.
- Ahmed, S., Rasul, M.G., Martens, W.N., Brown, R. and Hashib, M.A., (2010). Heterogenous photocatalytic degradation of phenols in wastewater: a review on current status and developments. *Desalination*, 261(1), pp.3-18.
- Ahsan Habib, M., Ismail, I., Mahmood, A. and Rafique Ullah, M., (2012). Photocatalytic decolorization of Brilliant Golden Yellow in TiO₂ and ZnO suspensions. *Journal of Saudi Chemical Society*, 16(4), pp.423-429

- Akkari, M., Aranda, P., Belver, C., Bedia, J., Ben Haj Amara, A. and Ruiz-Hitzky, E., (2018). Reprint of ZnO/sepiolite heterostructured materials for solar photocatalytic degradation of pharmaceuticals in wastewater. *Applied Clay Science*, 160, pp.3-8.
- Ali, K., Dwivedi, S., Azam, A., Saquib, K., Al-said, M.S., Alkhedhairy, A.A., (2016). Aloe vera extract functionalized zinc oxide nanoparticles as nanoantibiotics against multi-drug resistant clinical bacterial isolates, *J. Colloid Interface Sci* 472 (2016), pp.145–156
- Amani, M. and Ashrafu, M., (2015). Photocatalytic degradation of some organics dyes under solar light irradiation using TiO₂ and ZnO nanoparticles. *Nanochemistry Research*, 1(1), pp.79-86.
- Amna Adnan, 2010. Methods of Wastewater Treatment. [Online] Available through: <https://www.biotecharticles.com/Environmental-Biotechnology-Article/Methods-of-Wastewater-Treatment-353.html> [Accessed on 28 Jun 2018]
- Benhebal, H., Chaib, M., Salmon, T., Geens, J., Leonard, A., Lambert, S., Crine, M. and Heinrichs, B., (2013). Photocatalytic degradation of phenol and benzoic acid using zinc oxide powder prepared by the sol-gel process. *Alexandra Engineering Journal*, 52(3), pp.517-523.
- Bode, H.B., Kerkhoff, K., and Jendrossek, D., (2001). Bacterial Degradation of Natural and Synthetic Rubber. *Biomacromolecules*.2, pp.295-303.
- Buazar, F., Alipouryan, S., Kroushawi, F. and Hossieni, S. (2014). Photodegradation of odorous 2-mercaptobenzoxazole through zinc oxide/hydroxyapatite nanocomposite. *Applied Nanoscience*, 5(6), pp.719-729.
- Bystrov, V., Piccirillo, C., Tobaldi, D., Castro, P., Coutinho, J., Kopyl, S. and Pullar, R., (2016). Oxygen vacancies, the optical band gap (E_g) and photocatalysis of hydroxyapatite: Comparing modelling with measured data. *Applied Catalysis B: Environmental*, 196, pp.100-107

- Chakrabarti, S. and Dutta, B.K., (2004). Photocatalytic degradation of model textile dyes in wastewater using ZnO as semiconductor catalyst. *Journal of hazardous materials*, 112(3), pp.269-278
- Chamjangali, M.A. and Boroumand, S., (2013). Synthesis of flower-like Ag-ZnO nanostructure and its application in the degradation of methyl orange. *Journal of Brazil Chemical Society*, 24, pp. 1329-1338.I
- Chen. Y.C. and Lo, S.L., (2011). Effects of operational conditions of microwave-assisted synthesis on morphology and photocatalytic capability of zinc oxide. *Chemical engineering journal*, 170(2), pp.411-418.
- Chin, Y.H., Sin, J.C., Lam, S.Z. and Mohamed, A.R. (2018). Preparation of Nb₂O₅-decorated hierarchical porous ZnO microspheres with enhanced photocatalytic degradation of palm oil mill effluent. *Journal of Materials Science: Materials in Electronics*, 30(2), pp.1739-1750.
- Conserve Energy Future, 2018. What is Wastewater Treatment. [Online] Available through: <<https://www.conserve-energy-future.com/process-of-wastewater-treatment.php>> [Accessed on 28 Jun 2018]
- Daneshvar, N., Rasoulifard, M.H., Khataee, A.R. and Hosseinzadeh, F., (2007). Removal of CI Acid Orange 7 from aqueous solution by UV irradiation in the presence of ZnO nanopowder. *Journal of Hazardous Materials*, 143(1), pp.95-101.
- Department of Environment(DOE), 2012. River Water Pollution Sources [Website] Available through: <<https://www.doe.gov.my/portalv1/en/info-umum/punca-punca-kepada-pencemaran-air-sungai/278> > [Accessed on 26 Jun 2018]
- Delnavaz, M., Ayati, B., Ganjidoust, H. and Sanjabi, S., (2012). Kinetics study of photocatalytic process for treatment of phenolic wastewater by TiO₂ nanopowder immobilized on concrete surfaces. *Toxicological & Environmental Chemistry*, 94(6), pp.1086-1098.

- Djebbar, K., Zertal, A. and Sehili, T., (2006). Photocatalytic degradation of 2,4-Dichlorophenoxyacetic Acid and 4-Chloro-2-Methylephenoxyacetic Acid in Water by using TiO₂. *Environmental Technology*, 27(11), pp.1191-1197.
- Elumalai a, K., Velmurugan, S., Ravi, S., Kathiravan, V. and Adaikala Raj, G., (2015). Advanced Power Technology. *Bio-approach: Plant mediated synthesis of ZnO nanoparticles and their catalytic reduction of methylene blue and antimicrobial activity*, 26(6), pp.1639-1651.
- Elumalai, K., Velmurugan, S., Ravi, S., Kathiravan, V. and Ashokkumar, S., (2015). RETRACTED: Green synthesis of zinc oxide nanoparticles using Moringa oleifera leaf extract and evaluation of its antimicrobial activity. *Spectrochimica Acta Part A: Molecular and Biomolecular Spectroscopy*, 143, pp.158-164.
- Environment Pollution Centres, n.d. What Is Water Pollution? [magazine article] Available through: <https://www.environmentalpollutioncenters.org/water/> [Accessed 26 Jun 2018]
- Elaw.(n.d).Malaysia Environmental Quality Act 1974.[online] Available at: < <https://www.elaw.org/system/files/MalaysiaEQA1974.pdf> > [Accessed on 28 Jun 2018]
- Fluidinova, 2018. Hydroxyapatite. Available at: <https://www.fluidinova.com/hydroxyapatite-properties-uses-and-applications> [Accessed on 28 Jun 2018]
- Fu, L. and Fu, Z., (2015). Plectranthus amboinicus leaf extract–assisted biosynthesis of ZnO nanoparticles and their photocatalytic activity. *Ceramics International*, 41(2), pp.2492-2496.
- Ghoreishian, S.M., Badii, K., Norouzi,M., Rashidi,A., Montazer, M., Sadeghi, M. and Vafae,M., (2014). Decolorization and mineralization of an azo reactive dye using loaded nano-photocatalysts on spacer fabric: kinetic study and operational factors. *Journal of the Taiwan Institute of Chemical Engineers*, 45(5), pp.2436-2446.

- Ghule, L.A., Patil, A.A., Sapnar, K.B., Dhole, S.D. and Garadkar, K.M., (2011). Photocatalytic degradation of methyl orange using ZnO nanorods. *Toxicological & Environment Chemistry*, 93(4), pp.623-634.
- Giahi, M., Ghanbari, F., and Issazadeh, K., (2013). Photocatalytic Degradation of Nonionic Surfactant Using Zinc Oxide Nanoparticles. *Asian Journal of Chemistry*, 25(9), pp. 5047.
- Girish, K., (2014). Effect of Carbon Sources On the Biomass Build-Up and Degradation of Rubber Processing Industry Effluent. *International Journal of Applied Sciences and Biotechnology*, 2(4), pp.2091-2609.
- Gnanajobitha, G., Paulkumar, K., Vanaja, M., Rajeshkumar, S., Malarkodi, C., Annadurai, G. and Kannan, C., (2013). Fruit-mediated synthesis of silver nanoparticles using *Vitis vinifera* and evaluation of their antimicrobial efficacy. *Journal of Nanostructure in Chemistry*, 3(1), p.67.
- Guo, J., Dong, F., Zhong, S., Zhu, B., Huang, W. and Zhang, S., (2017). TiO₂-Hydroxyapatite Composite as a New Support of Highly Active and Sintering-Resistant Gold Nanocatalysts for Catalytic Oxidation of CO and Photocatalytic Degradation of Methylene Blue. *Catalysis Letters*, 148(1), pp.359-373.
- Hanada, T., (2009). Oxide and Nitride Semiconductors. *Advances in Materials Research*, pp.1-19.
- Hakim, L., Yaakob, Z., Puspasari, I. and Wan Daub, W.R., (2016). Hydroxyapatite-Supported Tri- Metallic Catalyst for hydrogen production from steam reforming of glycerol. *Jurnal Teknologi (Sciences & Engineering)* 78(5), pp.381-386.
- Hassani, A., Behnajady, M.A. and Rahbarfam, R., (2011). Effect of operational parameters on decolorization of Acid Yellow 23 from wastewater by UV irradiation using ZnO and ZnO/SnO₂ photocatalyst. *Desalination*, 271(1), pp.1636-1641.
- Hu, M., Yao, Z., Liu, X., Ma, L., He, Z. and Wang, X., (2018). Enhancement mechanism of hydroxyapatite for photocatalytic degradation of gaseous

- formaldehyde over TiO₂/hydroxyapatite. *Journal of the Taiwan Institute of Chemical Engineers*, 85, pp.91-97.
- Jafarirad, S., Mehrabi, M., Divband, B. and Kosari-Nasab, M., (2016). Biofabrication of zinc oxide nanoparticles using fruit extract of *Rosa canina* and their toxic potential against bacteria: A mechanistic approach. *Materials Science and Engineering: C*, 59, pp.296-302.
- Jai Shanker Pillai, H.P., Girish, K., (2014). Rubber processing industry effluent treatment using a bacterial consortium. *International Journal of Current Microbiology and Applied Sciences*. 3(10), pp.775-782.
- Jaworski, J., Cho, S., Kim, Y., Jung, J., Jeon, H., Min, B. and Kwon, K., (2013). Hydroxyapatite supported cobalt catalysts for hydrogen generation. *Journal of Colloid and Interface Science*, 394, pp.401-408.
- Jayamadhava, P., (2014). Synthesis of ZnO Nano Particle as an Alternative Catalyst for Photocatalytic Degradation of Brilliant Red Azo Dye. *American Journal of Environmental Protection*, 3(6), p.318.
- Jeffery Hays, 2013. Rubber in Malaysia [Online] Available through: <http://factsanddetails.com/southeast-asia/Malaysia/sub5_4e/entry-3702.html> [Accessed on 26 Jun 2018]
- Jiang, Y., Sun, Y., Liu, H., Zhu, F. and Yin, H., (2008). Solar photocatalytic decolorization of C.I. Basic Blue 41 in an aqueous suspension of TiO₂-ZnO. *Dyes and Pigments*, 78(1), pp.77-83.
- Kadhim, Q.A. & Sahan, Kassim & Ali, R.A. & Mahdi, R.J. & Kassim, N.A. & Jassim, A.N. & Alwan, R.M., (2015). Synthesis of zinc oxide nanoparticles via sol-gel route and their characterization. *Nanosci Nanotech*.5.1-6.
- Karthik, S., Siva, P., Balu, K., Suriyaprabha, R., Rajendran, V. and Maaza, M., (2017). *Acalypha indica*-mediated green synthesis of ZnO nanostructures under differential thermal treatment: Effect on textile coating, hydrophobicity, UV

- resistance, and antibacterial activity. *Advanced Powder Technology*, 28(12), pp.3184-3194.
- Kansal, S.K., Kaur, N. and Singh, S., (2009). Photocatalytic degradation of two commercial reactive dyes in aqueous phase using nanophotocatalysts. *Nanoscale research letters*, 4(7), p.709.
- Karthik, S., Siva, P., Shanmugam Balu, K., Suriyaprabha, R., Rajemdran, V., Maaza, M., (2017). *Advanced Power Technology: Acalypha indica*–mediated green synthesis of ZnO nanostructures under differential thermal treatment: Effect on textile coating, hydrophobicity, UV resistance, and antibacterial activity [e-journal] pp. 3184-3194.
- Kaur, J., Bansal, S. and Singhal, S., (2013). Photocatalytic degradation of methyl orange using ZnO nanopowders synthesized via thermal decomposition of oxalate precursor method. *Physica B: Condensed Matter*, 416, pp.33-38.
- Kazeminezhad, I. and Sadollahkhani, A., (2014). Photocatalytic degradation of Eriochrome Black-T dye using ZnO nanoparticles. *Materials Letters*, 120, pp.267-270.
- Khezrianjoo, S. and Revanasiddappa, H., (2013). Photocatalytic Degradation of Acid Yellow 36 Using Zinc Oxide Photocatalyst in Aqueous Media. *Journal of Catalysts*, 2013, pp.1-6.
- Kirchnerova, J., Herrera Cohen, M., Guy, C. and Klvana, D., (2005). Photocatalytic Oxidation of N-butanol under Fluorescent Visible Light lamp over commercial TiO₂ (Hombicat UV100 and Degussa P25). *Applied Catalyst A: General*, 282(1-2), pp.321-322.
- Kornochalart, N., Kantachote, D., Chaiprapat, S. and Techkarnjanaruk, S., (2014). Bioaugmentation of latex rubber sheet wastewater treatment with stimulated indigenous purple nonsulfur bacteria by fermented pineapple extract. *Electroic Joirnal of Biotechnology*. 17, pp.174-182.

- Krishnakumar, B. and Swaminathan, M., (2011). Influence of operational parameters on photocatalytic degradation of a genotoxic azo dye Acid Violet 7 in aqueous ZnO suspensions. *Spectrochimica Acta Part A: Molecular and Biomolecular Spectroscopy*, 81(1), pp.739-744.
- Krupa, A.N.D and Vimala, R., (2016). Evaluation of tetraethoxysilane (TEOS) sol-gel coatings, modified with green synthesized zinc oxide nanoparticles for combating microfouling, *Mater. Sci. Eng. C*. 61 pp.728–735
- Lakshmi, S., Bai R S, R., H, S. and Nidoni, U., (2017). A REVIEW STUDY OF ZINC OXIDE NANOPARTICLES SYNTHESIS FROM PLANT EXTRACTS. *Green Chemistry & Technology Letters*, 3(2), p.26.
- Lam, S.M., Sin, J.C., Abdullah, A.Z. and Mohamed, A.R., (2012): Degradation of wastewaters containing organic dyes photocatalysed by zinc oxide: a review, *Desalination and Water Treatment*, 41:1-3, 131-169
- Lam, S.M., Kee, M.C., and Sin, J.C., (2018). Influence of PVP surfactant on the morphology and properties of ZnO micro/nanoflowers for dye mixtures and textile wastewater degradation. *Materials Chemistry and Physics*, 212, pp.35-43.
- Lam, S.M., Low, X., Wong, K.A., and Sin, J.C., (2018). Sequencing coagulation–photodegradation treatment of Malachite Green dye and textile wastewater through ZnO micro/nanoflowers. *Chemical Engineering Communications*, 205(8), pp.1143-1156.
- Lee, S.L., Ho, L.N., Ong, S.A., Wong, Y.S., Voon, C.H., Khalik, W.F., Yusoff, N.A. and Nordin, N., (2017). A highly efficient immobilized ZnO/Zn photoanode for degradation of azo dye Reactive Green 19 in a photocatalytic fuel cell. *Chemosphere*, 166, pp.118-125.
- Lv, T., Pan, L., Liu, X. and Sun, Z., (2012). Enhanced photocatalytic degradation of methylene blue by ZnO- reduced graphene oxide-carbon nanotube composites synthesized via microwave-assisted reaction. *Catalysis Science & Technology*, 2(11), pp.2297-2301.

- Akkari, M., Aranda, P., Belver, C., Bedia, J., Ben Haj Amara, A., Ruiz-Hitzky, E., (2018). Applied Clay Science: Reprint of ZnO/sepiolite heterostructured materials for solar photocatalytic degradation of pharmaceuticals in wastewater [e-journal] pp. 3-8 Available through: < <https://www-sciencedirect-com.libezp2.utar.edu.my/science/article/pii/S0169131718300851>> [Accessed on 28 Jun 2018]
- Mazille, F., (2008). Advanced Oxidation Process. [online] Available at: <https://www.sswm.info/content/advanced-oxidation-processed> [Accessed 4 July 2017]
- Miao, J., Jia, Z., Lu, H.B., Habibi, D. and Zhang, L.C., (2014). Heterogenous photocatalytic degradation of mordant black 11 with ZnO nanoparticles under UV-Vis light. *Journal of the Taiwan of Chemical Engineers*, 45(4), pp.1636-1641.
- Department of Environment, (2012). [ebook] Malaysia: Malaysia Environmental Quality Report 2012, p.83. Available at: [https://enviro.doe.gov.my/ekmc/wp-content/uploads/2016/08/1391999272-1391998509-Malaysia%20Environment%20Report%202012\(NEW\).pdf](https://enviro.doe.gov.my/ekmc/wp-content/uploads/2016/08/1391999272-1391998509-Malaysia%20Environment%20Report%202012(NEW).pdf) [Accessed 20 Apr. 2019].
- Mohammadi, M., Man, H.S., Hassan, M.A., Phang, L.Y., (2010). Treatment of wastewater from rubber industry in Malaysia. *African Journal of Biotechnology*. 9(38), pp.6233-6243.
- Mohsin, D., Juda, A. and Mashkour, M., (2013). Thermodynamic and Kinetic Study for Aromatic Rings Effect on The Photooxidation rate. *International Journal of Engineering & Technology IJET-IJENS*, 13(4), 34-40.
- Mori, K., Hara, T., Mizugaki, T., Ebitani, K. and Kaneda, K., (2004). Hydroxyapatite-Supported Palladium Nanoclusters: A Highly Active Heterogeneous Catalyst for Selective Oxidation of Alcohols by Use of Molecular Oxygen. *American Chemical Society*. 126. Pp.10657-10666.
- Munter, R., (2010). ChemInform Abstract: Advanced Oxidation Processes: Current Status and Prospects. *ChemInform*, 32(41), pp.59.80.

- Palaez, M., Nolan, N.T., Pillai, S.C., Seery, M.K., Falaras, P., Kontas, A.G., Dunlop, P.S., Hamilton, J.W., Bayrne, J.A., O'shea, K. and Entezari, M.H., (2012). A review on the visible light active titanium dioxide photocatalysts for environmental applications. *Applied Catalysis B: Environmental*, 125, pp.331-349.
- Palominos, R., Mondaca, M., Giraldo, A., Penuela, G., Perez-Moya, M. and Mansilla, H., (2009). Photocatalytic oxidation of the antibiotic tetracycline on TiO₂ and ZnO suspensions. *Catalysis Today*, 144(1-2), pp100-105
- Pirsaheb, M., Shahmoradi, B., Beikmohammadi, M., Azizi, E., Hossini, H. and Md Ashraf, G., (2017). Photocatalytic Degradation of Aniline from Aqueous Solutions under sunlight illumination using immobilized Cr.ZnO nanoparticles. *Scientific Report*, 7(1).
- Rajamanickam, D. and Shanthi, M., (2016). Photocatalytic degradation of an organic pollutant by Zinc Oxide- Solar Process. *Arabian Journal of Chemistry*, 9, pp. S1858-S1868.
- Raliya, R. and Tarafdar, J., (2013). ZnO Nanoparticle Biosynthesis and Its Effect on Phosphorous-Mobilizing Enzyme Secretion and Gum Contents in Clusterbean (*Cyamopsis tetragonoloba* L.). *Agricultural Research*, 2(1), pp.48-57.
- Ramesh, M., Anbuvaran, M. and Viruthagiri, G., (2015). Green synthesis of ZnO nanoparticles using *Solanum nigrum* leaf extract and their antibacterial activity. *Spectrochimica Acta Part A: Molecular and Biomolecular Spectroscopy*, 136, pp.864-870.
- Ramanan, G. and V.N., (2015). Treatment of Waste Water from Natural Rubber Processing Plant. *International Journal of Scientific Engineering and Research (IJSER)*, pp.2347-3878.
- Rao, D.G., Senthilkumar, R., Anthony Byrne, J., Feroz, S., (2012). Wastewater Treatment: Advanced Processes and Technologies. IWA Publishing, 49.

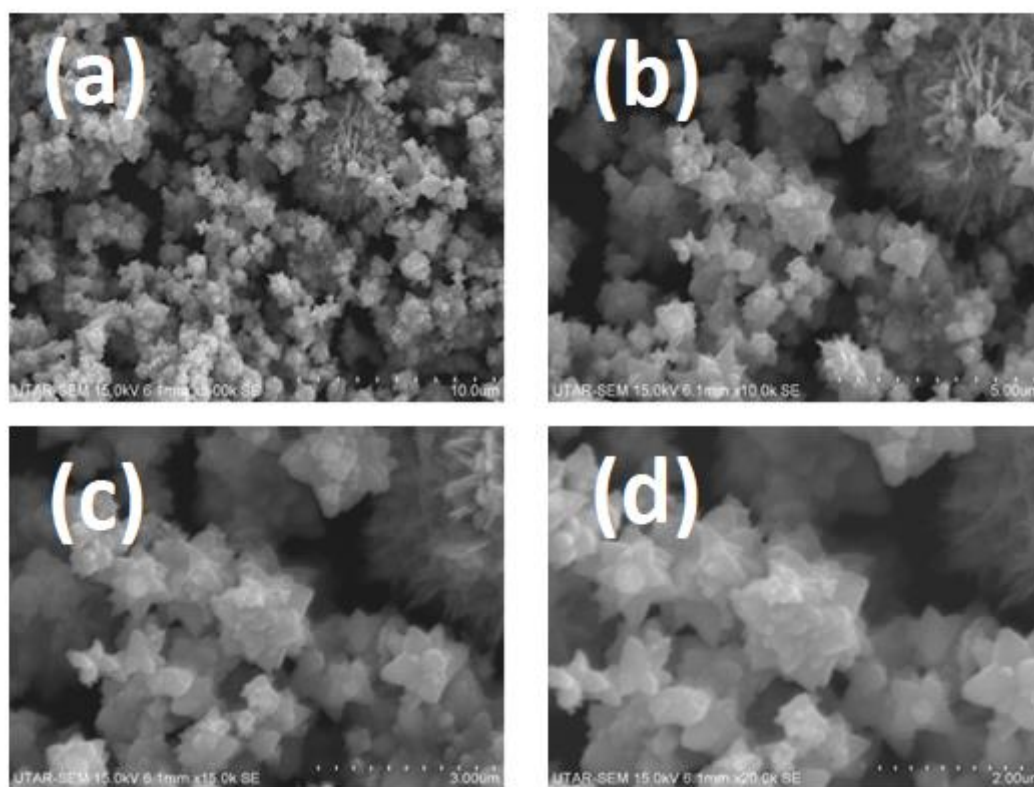
- Regulska, E., Brus, D.M., Rodziewicz, P., Sawicka, S. and Karpinska, J., (2016). Photocatalytic degradation of hazardous Food Yellow 13 in TiO₂ and ZnO aqueous and river water suspensions. *Catalysis Today*, 266, pp.72-81.
- Rogé, V., Guignard, C., Lamblin, G., Laporte, F., Fechete, I., Garin, F., Dinia, A. and Lenoble, D., (2018). Photocatalytic degradation behavior of multiple xenobiotics using MOCVD synthesized ZnO nanowires. *Catalysis Today*, 306, pp.215-222.
- Romat, M., (2010). Photocatalysis offers a concrete solution to one of the major problems our society has to face: environmental pollution. [Online] Available at: <<http://www.newwayssustainability.org/en/2015/11/17/applications-and-advantages-of-photocatalysis/>> [Accessed on 28 Jun 2018]
- Saikia, L., Bhuyan, D., Saikia, M., Malakar, B., Dutta, D.K. and Sengupta, P., (2015). Photocatalytic performance of ZnO nanomaterials for self-sensitized degradation of malachite green dye under solar light. *Applied Catalysis A: General*, 490, pp.42-49.
- Samir. R., Essam, T., Ragab, Y. and Hashem, A., (2015). Enhanced photocatalytic biological degradation of 2,4 dichlorophenoxyacetic acid. *Bulletin of Faculty of Pharmacy, Cairo Univeristy*, 53(2), pp.77-82.
- Santhoshkumar, J., Rajeshkumar, S. and Venkat Kumar, S., (2017). Resources Efficient Technologies. *Synthesis of zinc oxide nanoparticles using plant leaf extract against urinary tract infection pathogen*, 3(4), pp.459-465.
- Sin, J.C., Lam, S.M., Lee, K.T. and Mohamed, A.R., (2013). Preparation and photocatalytic properties of visible light-driven samarium-doped ZnO nanorods. *Ceramics International*, 39(5), pp.5833-5843.
- Sohrabnezhad, S. and Seifi, A. (2016). The green synthesis of Ag/ZnO in montmorillonite with enhanced photocatalytic activity. *Applied Surface Science*, 386, pp.33-40.

- Spitia, P., Soares, N., Coimbra, J., de Andrade, N., Cruz, R. and Medeiros, E., (2012). Zinc Oxide Nanoparticles: Synthesis, Antimicrobial Activity and Food Packaging Applications. *Food and Bioprocess Technology*, 5(5), pp.1447-1464.
- Uti, E., Laouedj, N. and Ahmed, B. (2011). ZnO- Assisted Photocatalytic Degradation of Congo Red and Benzopurpurine 4B in Aqueous Solution. *Journal of Chemical Engineering & Process Technology*, 02(3).
- Vanathi, P., Rajiv, P., Narendhran, S., Rajeshwari, S., Rahman, P. and Venckatesh, R., (2014). Biosynthesis and characterization of phyto mediated zinc oxide nanoparticles: A green chemistry approach. *Materials Letters*, 134, pp.13-15.
- Venugopal, A., (2003). Hydroxyapatite as a novel support for gold and ruthenium catalysts Behaviour in the water gas shift reaction. *Applied Catalysis A: General*, 245(1), pp.137-147.
- V. Rogé, C. Guignard, G. Lamblin, F. Laporte, I. Fechete, F. Garin, A. Dinia and D. Lenoble, (2016). Catalysis Today: Photocatalytic degradation behavior of multiple xenobiotics using MOCVD synthesized ZnO nanowires [e-database] pp. 215-222.
- Wahab, R., Ansari, S., Kim, Y., Seo, H., Kim, G., Khang, G. and Shin, H. (2007). Low temperature solution synthesis and characterization of ZnO nano-flowers. *Materials Research Bulletin*, 42(9), 1640-1648.
- Xiong, G., Pal, U., Serrano, J., Ucer, K. and Williams, R. (2006). Photoluminescence and FTIR study of ZnO nanoparticles: the impurity and defect perspective. *phys. stat. sol. (c)*, 3(10), 3577-3581.
- Yang, C., Dong, W., Cui, G., Zhao, Y., Shi, X., Xia, X., Tang, B. and Wang, W., (2017). Highly –efficient photocatalytic degradation of methylene blue by PoPD-modified TiO₂ nanocomposites due to photosensitization-synergetic effect of TiO₂ with PoPD. *Scientific Reports*, 7(1).
- Yang, Z., Gong, X. and Zhang, C., (2010). Recyclable Fe₃O₄/hydroxyapatite composite nanoparticles for photocatalytic applications. *Chemical Engineering Journal*, 165(1), pp.117-121.

- Yuvakkumar, R., Suresh, J., Nathanael A.J., Sundrarajan, M., Hong, S.I., (2014). Novel green synthetic strategy to prepare ZnO nanocrystals using rambutan (*Nephelium lappaceum* L.) peel extract and its antibacterial applications, *Mater. Sci. Eng. C*. 41 pp.17–27.
- Zhao, X.Y., Zhu, Y.J., Zhao, J., Lu, B.Q., Chen, F., Qi, C., Wu, J., (2014). Hydroxyapatite nanosheet-assembled microspheres: hemoglobin-templated synthesis and adsorption for heavy metal ions. *J Colloid Interface Sci* 416:11–18.
- Zhai, J., Tao, X., Pu, Y., Zeng, X.F. and Chen, J.F., (2010). Core/Shell structured ZnO/SiO₂ nanoparticles: preparation, characterization and photocatalytic property. *Applied Surface Science*, 257(2), pp.393-397.

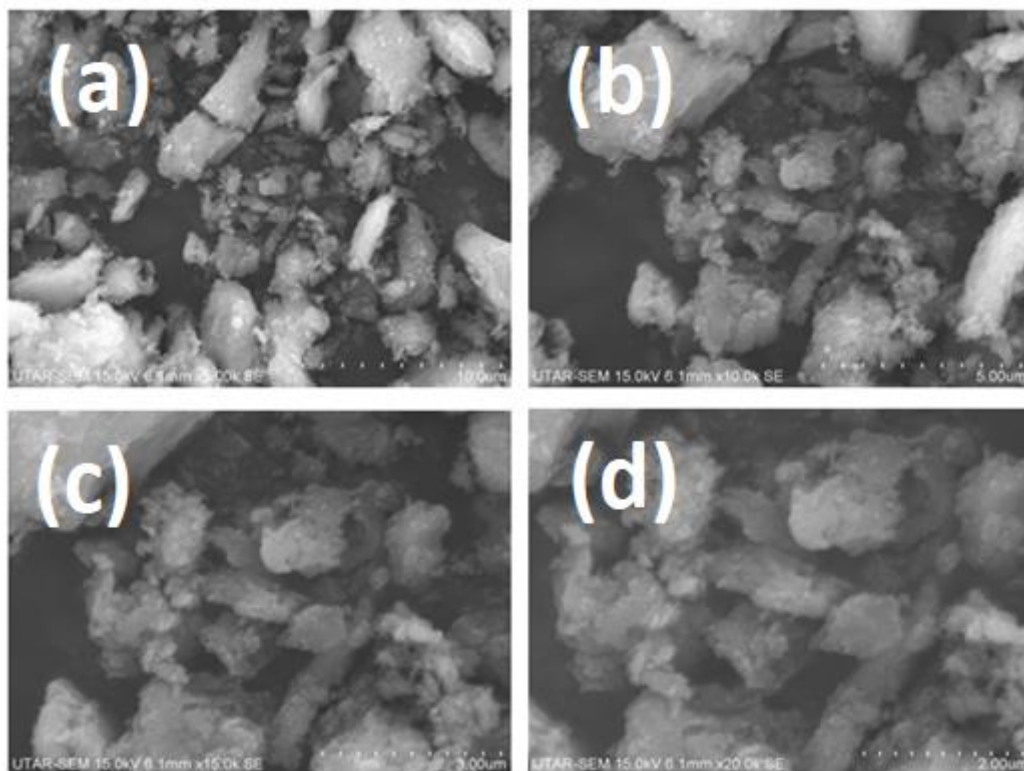
APPENDICES

APPENDIX A



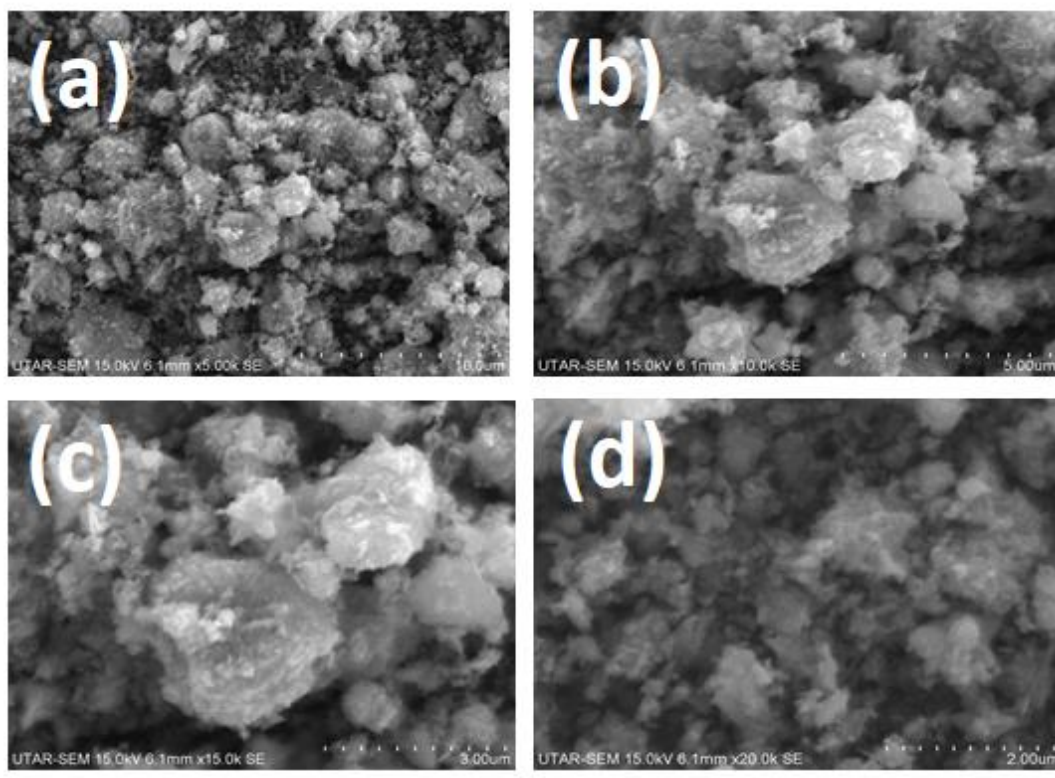
Appendix A: SEM image of Corn Husk ZnO with different magnification. (a) x5,000 (b) x10,000 (c) x15,000 (d) x20,000

APPENDIX B



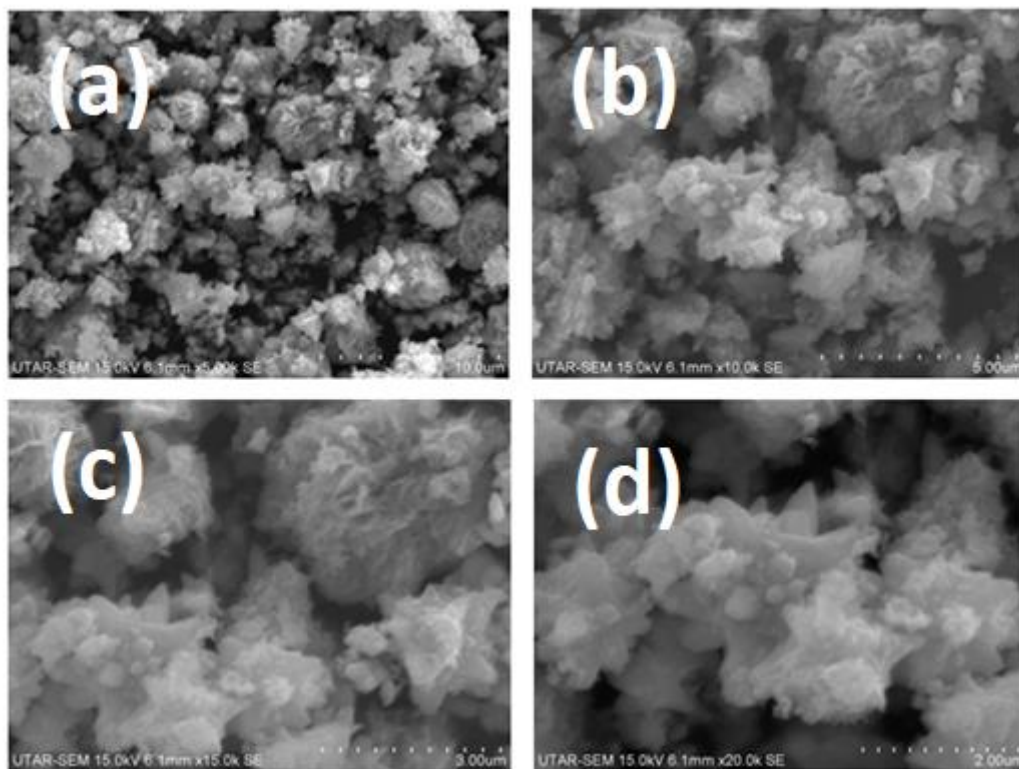
Appendix B: SEM image of HAp with different magnification. (a) x5,000 (b) x10,000 (c) x15,000 (d) x20,000

APPENDIX C



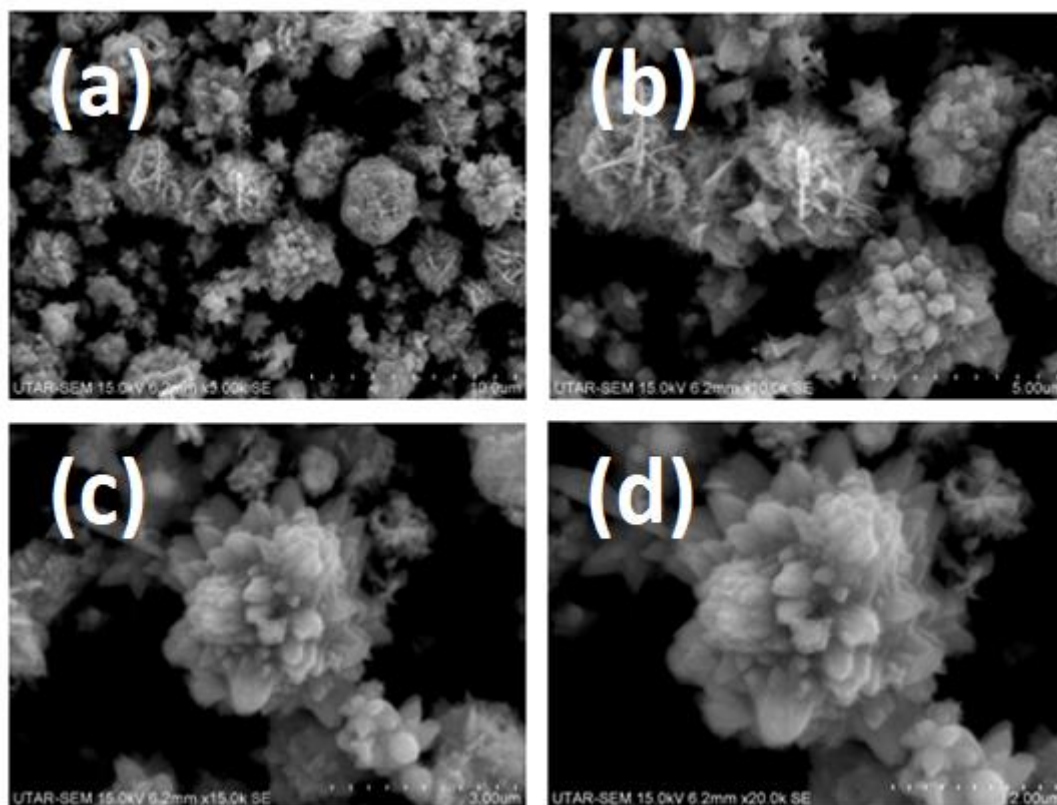
Appendix C: SEM image of ZnO-20%HAp with different magnification. (a) x5,000 (b) x10,000 (c) x15,000 (d) x20,000

APPENDIX D



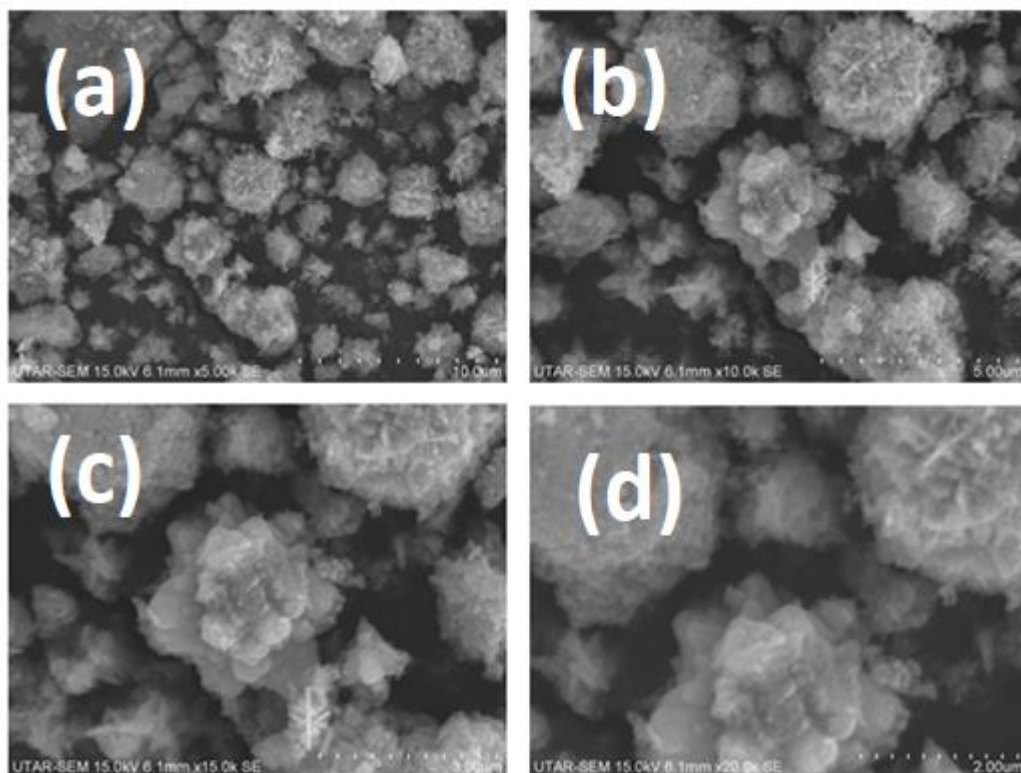
Appendix D: SEM image of ZnO-30%HAp with different magnification. (a) x5,000 (b) x10,000 (c) x15,000 (d) x20,000

APPENDIX E



Appendix E: SEM image of ZnO-40%HAp with different magnification. (a) x5,000 (b) x10,000 (c) x15,000 (d) x20,000

APPENDIX F



Appendix F: SEM image of ZnO-50%HAp with different magnification. (a) x5,000 (b) x10,000 (c) x15,000 (d) x20,000